Liquid Crystals
Publication details, including instructions for authors and subscription information:
http://www.informaworld.com/smpp/title~content=t713926090

Thermotropic columnar mesophases of wedge-shaped benzenesulfonic acid mesogens

Uwe Beginn[a]; Linglong Yan[b]; Sergei N. Chvalun[c]; Maxim A. Shcherbina[c]; Artem Bakirov[c]; Martin Möller[b]
[a] Organic Materials Chemistry, Institute for Chemistry, University Osnabrueck, D-49069 Osnabrueck, Germany [b] Institute of Technical and Macromolecular Chemistry, RWTH Aachen and DWI e.V., D-52056 Aachen, Germany [c] Karpov Institute of Physical Chemistry, 103064 Moscow, Russia

To cite this Article Beginn, Uwe , Yan, Linglong , Chvalun, Sergei N. , Shcherbina, Maxim A. , Bakirov, Artem and Möller, Martin(2008) 'Thermotropic columnar mesophases of wedge-shaped benzenesulfonic acid mesogens', Liquid Crystals, 35: 9, 1073 — 1093
To link to this Article: DOI: 10.1080/02678290802376107
URL: http://dx.doi.org/10.1080/02678290802376107

Liquid Crystals,
Vol. 35, No. 9, September 2008, 1073–1093

Taylor & Francis
Taylor & Francis Group

Thermotropic columnar mesophases of wedge-shaped benzenesulfonic acid mesogens

Uwe Beginn[a]*, Linglong Yan[b], Sergei N. Chvalun[c], Maxim A. Shcherbina[c], Artem Bakirov[c] and Martin Möller[b]

[a]*Organic Materials Chemistry, Institute for Chemistry, University Osnabrueck, Barbarastr. 7, D-49069 Osnabrueck, Germany;* [b]*Institute of Technical and Macromolecular Chemistry, RWTH Aachen and DWI e.V., Pauwelsstr. 8, D-52056 Aachen, Germany;* [c]*Karpov Institute of Physical Chemistry, Vorontsovo Pole 10, 103064 Moscow, Russia*

(Received 8 March 2008; final form 29 July 2008)

The synthesis and characterisation are reported of two groups of new amphiphilic sulfonate compounds, 2,3,4-tris(dodecyloxy)benzenesulfonates, 2,3,4-tris(dodecyloxy)benzenesulfonamide and the isomeric 3,4,5-tris(dodecyloxy)benzenesulfonates. As revealed by a combination of thermo-optical microscopy, differential scanning calorimetry and X-ray scattering techniques, the occurrence of mesophases is controlled by the radius of the cation and the symmetry of the molecule. The sulfonates exhibited a rich phase behaviour involving cubic, ordered and disordered columnar mesophases, depending on the counter ion and the type of substitution. It is proposed that the term 'cunitic' molecules should be introduced as a class descriptor for wedge-shaped molecules and their columnar phases.

Keywords: columnar mesophases; wedge-shaped sulfonate amphiphiles; cunitic molecules

1. Introduction

The rapid development of material science during recent decades has involved not only the discovery of new materials, but also improved control over the materials 'mesostructure', i.e. structures on the length scale 1–100 nm. Improved control of microstructures has allowed preparation of crystalline, transparent polypropylene (*1*), control of the birefringence of plastic materials by selective orientation of micro-crystalline units (*2*) and formation of 'nanocomposites' from layered silicates and macromolecular materials with enhanced stiffness and reduced permeability and flammability (*3*). There is, however, much still to learn on the possibilities that are offered by the perfect control of the materials mesostructure: self-organisation of functional sub-units to complex machinery like superstructures is also known to be the building principles of viruses, microtubuli and membrane transport channels (*4*).

Most of biological sub-units consist of protein chains that cannot yet be copied by chemists, because of the lack of a perfect sequential synthesis technique. However, self-organisation is not limited to functional macromolecules, but is well established for compounds of low molecular weight (*5*).

Among numerous examples of self-organising low molecular weight compounds (*6*), wedge-shaped amphiphilic molecules have been found to be versatile building blocks that generate cylindrical superstructures. The importance of an amphiphilic molecular structure and the required hydrophobic/hydrophilic balance to control thermotropic mesophase types has been demonstrated for polyhydroxy amphiphiles (*7*).

In particular, the column structure can be controlled to confine the tips of the molecular wedges along the column centres, whereas the outer rim of the column structures is composed of the molecular moieties of the bulky sides of the wedges (*8, 9, 10*). This property makes the columns ideal supramolecular building blocks for generating transport channels (*11, 12, 13, 14*), molecular cables or photon transport devices. Since most of these applications require a maximum of transport active units per cross-section, as well as a minimum of tortuosity along the transport path, the arrangement of the supramolecular columns into columnar mesophases is an important pre-requisite for the design of an active transport material.

We have focused our interest on columnar structures containing sulfonate groups in their interior, because such structures are considered to be ideal models for the transport phases found in perfluorinated sulfonate membranes (*15*). The first examples of molecular wedges bearing sulfonate salt tips and exhibiting columnar mesophases were described in previous papers (*16, 17*). These sulfonate wedges were preferably used to complex polybases and generate discrete supramolecular cylinder structures (*18*).

In this paper, a systematic relationship between the mesophase types and the symmetry of the molecular wedges as well as the ratio of the size of the polar tip of the wedges is presented. For this

*Corresponding author. Email: ubeginn@uni-osnabrueck.de

ISSN 0267-8292 print/ISSN 1366-5855 online

DOI: 10.1080/02678290802376107
http://www.informaworld.com

study, a synthetic path was developed to obtain 2,3,4-tris(dodecyloxy)benzenesulfonates and the isomeric 3,4,5-tris(dodecyloxy)benzenesulfonates.

2. Experimental

Techniques

^{1}H NMR (300 MHz) and ^{13}C NMR (75 MHz) spectra were recorded on a Bruker DPX-300 spectrometer with tetramethylsilane (TMS) as internal standard in deuterated chloroform at 20°C.

Differential scanning calorimetry (DSC) measurements were performed on samples of about 5 mg to 10 mg. Phase transitions were measured on a Netzsch DSC 204 'Phoenix' differential scanning calorimeter. In all cases, the heating and cooling rates were $10^\circ C\,min^{-1}$. Indium and cyclohexane were used as calibration standards. Phase transitions are reported as the maxima or minima temperatures of the respective endo- or exothermic signals.

For thermo-optical polarising microscopy, a Zeiss AXIOPLAN 2 polarising microscope, equipped with a Mettler FP 80 hot stage was used. Pictures were taken using a digital Zeiss AxioCam MRC4 camera with a resolution of 4 megapixels in combination with Zeiss AxioVision software.

X-ray scattering.

Small angle X-ray scattering (SAXS) data were recorded using a Kratky block camera with Ni-filtered Cu K_α radiation. The diverging and receiving slits were both 100 µm wide, providing a high resolution; the width of the primary beam was $3.3 \times 10^{-2}\,nm^{-1}$. The scattered intensity was measured with an angular step of $1.2 \times 10^{-2}\,nm^{-1}$ in the vicinity of the narrow intense 10 reflection, and with $2.4 \times 10^{-2}\,nm^{-1}$ increments over the rest of region covered. Exposure times were selected to be between 100 and 300 s, depending on the relative intensity of the reflections. The phase behaviour of all compounds was studied in the temperature interval from 20 to 250°C with an accuracy of 1°C.

Materials

1,2,3-Trihydroxybenzene (99+%, Aldrich), 1-bromododecane (99+%, Aldrich), potassium carbonate (97%, Aldrich), sulfuric acid (95~97%, Merck), thionyl chloride (99%, Merk), ammonia gas (Merck), methyllithium (Aldrich), sodium methanolate (ACS reagent), potassium methanolate (ACS reagent), caesium hydroxide (97%, Aldrich), pyridine (97%, Aldrich), tetramethylammonium hydroxide (0.1M in methanol, Aldrich), tetraethylammonium hydroxide (0.1M in methanol, Aldrich), tetrabutylammonium hydroxide (0.1M in methanol, Aldrich), sodium sulfite (ACS reagent, Merck), sodium hydroxide (ACS reagent), hydrochloric acid (0.1 M, ACS reagent), barium acetate (99%, Fluka), Amberlite IR120 (Fluka), lithium carbonate (99+%, Aldrich), sodium carbonate (ACS reagent), potassium carbonate (ACS reagent), caesium carbonate (99+%, Aldrich) and 11-bromo-1-undecene (95%, Aldrich) were used as received. Ethanol, methanol, acetone, diethylether, *n*-hexane, toluene, ethyl acetate, tetrahydrofuran, dichloromethane, isopropyl ether were all ACS reagents and used as received. *N*,*N*-Dimethylformamide was dried over calcium hydride for 12 h and distilled under vacuum.

Syntheses

*1,2,3-Tris(dodecyloxy)benzene (**1**).*

Under a nitrogen atmosphere, 1,2,3-trihydroxybenzene (11.0 g, 0.08 mol) and K_2CO_3 (55.5 g, 0.4 mol) were mixed with 125 ml freshly dried DMF in a 250 ml three-necked flask equipped with a magnetic stirrer. At 60°C, 1-bromododecane (55.2 ml, 0.23 mol) was added dropwise. The reaction mixture was stirred for 5 h at 60°C and subsequently slowly poured into 600 ml of ice water. The precipitate was isolated by filtration and dried in vacuum. The crude product was recrystallised from 300 ml acetone three times to give a white powder of **1**. Yield: 38.3 g≅76%. M.p. 39–40°C [lit. (*8*) 39.5–40.5°C]. TLC (20/1 hexane/ethylacetate): R_f=0.68. ^{1}H NMR (300 MHz, $CDCl_3$, 20°C, TMS): δ 0.88 (t, 9H, CH_3, J=6.6 Hz), 1.26 (overlapped peaks, 48H, $CH_3(CH_2)_8$), 1.47 (m, 6H, $O(CH_2)_2CH_2$), 1.78 (m, 6H, OCH_2CH_2), 3.90 (overlapped t, 6H, OCH_2, J=6.3 Hz), 6.55 (d, 2H, 4,6-benzene-*H*, J=8.1 Hz), 6.90 (t, 1H, 5-benzene-*H*, J=8.4 Hz). ^{13}C NMR (75 MHz, $CDCl_3$, 20°C, TMS): δ 14.1 (CH_3), 22.7 (CH_3CH_2), 26.1 ($OCH_2CH_2CH_2$), 29.4 ($CH_3CH_2CH_2CH_2$), 29.5 ($CH_3CH_2CH_2CH_2(CH_2)_5$, 29.9 (1,3-OCH_2CH_2), 30.3 (2-OCH_2CH_2), 31.9 ($CH_3CH_2CH_2$), 69.0 (1,3-OCH_2), 73.3 (2-OCH_2O), 106.7 (4,6-benzene-*C*), 123.1 (5-benzene-*C*), 138.4 (2-benzene-*C*), 153.4 (1,3-benzene-C).

*2,3,4-Tris(dodecyloxy)benzenesulfonic acid (**2**).*

Under a nitrogen atmosphere, **1** (1.2 g, 2.0 mmol) was added to 10 ml concentrated sulfuric acid (95–97%) at 0°C. The reaction suspension was stirred for 2 h while the temperature of the water bath was gradually increased to 20°C. The suspension was poured slowly into 50 ml ice water. The resulting light-yellow suspension was kept at 4°C for 1 h and the precipitate was isolated by filtration and pre-dried in vacuum.

The crude product was recrystallised from 30 ml acetone at 4°C three times and dried in vacuum to yield a white powder. Yield: 1.3 g≅88.7%. M.p. 65.0–65.5°C. ^{1}H NMR (300 MHz, $CDCl_3$, 20°C, TMS): δ 0.88 (t, 9H, CH_3, J=6.7 Hz), 1.27 (overlapped peaks, 48H, $CH_3(CH_2)_8$), 1.45 (m, 6H, $O(CH_2)_2CH_2$), 1.83 (m, 6H, OCH_2CH_2), 4.00 (overlapped t, 4H, 3- and 4-OCH_2), 4.29 (t, 2H, 2-OCH_2, J=6.98 Hz), 6.69 (d, 1H, 5-benzene-*H*, J=9.06 Hz), 7.54 (d, 1H, 6-benzene-*H*, J=8.85 Hz). ^{13}C NMR (75 MHz, $CDCl_3$, 20°C, TMS): δ 14.13, 22.70, 25.77, 26.10, 29.11, 29.39, 29.72, 30.00, 30.29, 31.94, 73.96, 75.77, 107.40, 123.20, 124.78, 141.89, 149.73, 157.79. IR (KBr, cm^{-1}): 3435.11 (s, broad), 2956.86 (m), 2917.63 (vs), 2851.29 (s), 1732.56 (w), 1631.30 (w), 1582.85 (w), 1486.22 (w), 1466.57 (m), 1441.26 (w), 1380.14 (w), 1304.58 (w), 1281.34 (w), 1226.56 (m), 1162.99 (w), 1087.42 (s), 1041.04 (w), 885.31 (w), 802.42 (w), 787.36 (w), 719.54 (w), 709.03 (w), 691.90 (w), 634.69 (w), 606.35 (w), 578.87 (w), 531.66 (w). Elemental analysis: calculated for $C_{42}H_{78}O_6S$ (wt %), C 71.04, H 10.93; found, C 69.13, H 11.32.

*2,3,4-Tris(dodecyloxy)benzenesulfonyl chloride (**3**).*

2 (1.0 g, 1.4 mmol) was dissolved in 150 ml freshly dried dichloromethane under nitrogen protection. A catalytic amount (0.5 ml) of DMF was added, followed by dropwise addition of (0.12 ml, 1.55 mmol) thionyl chloride at 0°C. The reaction mixture was stirred at room temperature for 1**2** h, the solvent was removed under reduced pressure and the obtained compound was dried. The product was used without further purification. ^{1}H NMR (300 MHz, $CDCl_3$, 20°C, TMS): δ 0.88 (overlapped t, 9H, CH_3, J=6.60 Hz), 1.26 (overlapped peaks, 54H, $CH_3(CH_2)_9$), 1.83 (m, 6H, OCH_2CH_2), 3.96 (tetra, 4H, 3- and 4-OCH_2, J=6.06 Hz), 4.19 (t, 2H, 2-OCH_2, J=6.98 Hz), 6.59 (d, 1H, 5-benzene-*H*, J=8.67 Hz), 7.55 (d, 1H, 6-benzene-*H*, J=8.67 Hz). ^{13}C NMR (75MHz, $CDCl_3$, 20°C, TMS): δ=14.12, 22.70, 25.89, 26.10, 29.22, 29.40, 29.65, 29.70, 29.76, 31.94, 73.74, 74.81, 106.63, 123.74, 142.23, 151.18, 156.71, 165.07.

*2,3,4-Tris(dodecyloxy)benzenesulfonamide (**4**).*

Under nitrogen protection, **3** (1.0 g, 1.4 mmol) was dissolved in 50 ml of a freshly prepared saturated solution of ammonia in THF. The reaction mixture was stirred at room temperature for 7 days; subsequently the solvent was removed under the vacuum and the resulting compound was freeze-dried to yield **4**. Yield: 0.7 g≅82.2%. M.p. 55.5°C. TLC (6/1 ethylacetate/methanol): R_f=0.23. ^{1}H NMR (300 MHz, $CDCl_3$, 20°C, TMS): δ 0.88 (overlapped t, 9H, CH_3), 1.26 (overlapped peaks, 54H, $CH_3(CH_2)_9$), 1.69 (m, 6H, OCH_2CH_2), 3.82 (broad, 4H, 3- and 4-OCH_2), 4.05 (broad, 2H, 2-OCH_2), 6.28 (broad, 1H, 5-benzene-*H*), 7.34 (broad, 1H, 6-benzene-*H*). ^{13}C NMR (75 MHz, $CDCl_3$, 20°C, TMS): δ 14.12, 22.71, 26.27, 29.44, 29.62, 29.80, 31.96, 31.96, 73.42, 106.7, 139.52, 140.03, 152.99. Elemental analysis: calculated for $C_{42}H_{79}NO_5S$ (wt %), C 71.03, H 11.21, N 1.97; found, C 68.81, H 11.93, N 1.72.

*Lithium 2,3,4-tris(dodecyloxy)benzenesulfonate (**5**).*

Under nitrogen atmosphere and at room temperature, 0.2 ml (0.32 mmol) of a 1.6 mol l^{-1} solution of methyllithium in diethyl ether was added to 5 ml of a freshly prepared solution of compound **2** (227.6 mg, 0.32 mmol) in absolute diethyl ether. The reaction mixture was stirred for 2 h; subsequently all volatiles were removed in a membrane pump vacuum. The obtained solid was dried at 40°C under vacuum to yield a white powder of **5**. Yield: 0.2 g≅87%. M.p. −11.1°C (by DSC). TLC (6/1 ethyl acetate/methanol): R_f=0.45. ^{1}H NMR (300 MHz, $CDCl_3$, 20°C, TMS): δ 0.88 (t, 9H, CH_3, J=6.23 Hz), 1.26 (overlapped peaks, 54H, $CH_3(CH_2)_9$), 1.77 (m, 6H, OCH_2CH_2), 3.84 (broad, 4H, 3- and 4-OCH_2), 4.08 (broad, 2H, 2-OCH_2), 6.34 (broad, 1H, 5-benzene-*H*), 7.34 (d, 1H, 6-benzene-*H*, J=8.28 Hz). ^{13}C NMR (75 MHz, $CDCl_3$, 20°C, TMS): δ 14.12, 22.72, 25.75, 26.33, 29.44, 29.55, 29.81, 30.53, 31.99, 32.04, 68,62, 73.67, 106.85, 123.74, 128.96, 141.82, 150.02, 155.73. Elemental analysis: calculated for $C_{42}H_{77}LiO_6S{\cdot}H_2O$ (wt %), C 68.63, H 10.83; found, C 68.28, H 10.97.

*Sodium 2,3,4-tris(dodecyloxy)benzenesulfonate (**6**).*

Under a nitrogen atmosphere, 19.0 mg (0.35 mmol) sodium methoxide were dissolved in 5 ml freshly dried methanol. Subsequently, 250 mg (0.35 mmol) of compound **2** were added, the reaction mixture was stirred vigorously for 2 h at room temperature and all volatiles were removed in a membrane pump vacuum. The obtained solid was freeze-dried with benzene under vacuum to yield a white powder of **6**. Yield: 0.21 g≅82%. M.p. −3.0°C (by DSC). TLC (6/1 ethyl acetate/methanol): R_f=0.34. ^{1}H NMR (300 MHz, $CDCl_3$, 20°C, TMS): δ 0.88 (overlapped t, 9H, CH_3), 1.26 (overlapped peaks, 54H, $CH_3(CH_2)_9$), 1.67 (broad, 6H, $O(CH_2)_2CH_2$), 3.79 (broad, 4H, 2,4-OCH_2), 4.03 (broad, 2H, 3-OCH_2), 6.18 (broad, 1H, 5-benzene-*H*), 7.28 (broad, 1H, 6-benzene-*H*). ^{13}C NMR (75MHz, $CDCl_3$, 20°C, TMS): δ=14.12, 22.74, 25.74, 26.42, 29.51, 29.60, 29.70, 29.95, 30.63, 32.01, 68,54, 73.47, 75.42, 106.61, 123.85, 128.90, 141.77, 150.20, 155.30. Elemental analysis: calculated for $C_{42}H_{77}NaO_6S{\cdot}H_2O$ (wt %), C 67.16, H 10.59; found, C 67.32, H 11.16.

*Potassium 2,3,4-tris(dodecyloxy)benzenesulfonate (**7**).*

Under a nitrogen atmosphere, 61.6 mg (0.88 mmol) potassium methoxide were dissolved in 10 ml freshly dried methanol. Subsequently, 625.4 mg (0.88 mmol) of compound **2** were added and the reaction mixture was stirred vigorously for 2 h at room temperature. Subsequently all volatiles were removed in a membrane pump vacuum and the obtained solid was freeze dried with benzene under vacuum to yield a white powder of **7**. Yield: 0.62 g≅94%. M.p. 17.8°C (by DSC). TLC (6/1 ethyl acetate/methanol): R_f=0.16. ^{1}H NMR (300 MHz, $CDCl_3$, 20°C, TMS): δ 0.88 (overlapped t, 9H, CH_3), 1.26 (overlapped peaks, 54H, $CH_3(CH_2)_9$), 1.75 (m, 6H, OCH_2CH_2), 3.84 (broad, 4H, 3- and 4-OCH_2), 4.07 (broad, 2H, 2-OCH_2), 6.29 (d, 1H, 5-benzene-*H*, *J*=8.28 Hz), 7.35 (d, 1H, 6-benzene-*H*, *J*=8.70 Hz). ^{13}C NMR (75 MHz, $CDCl_3$, 20°C, TMS): δ 14.12, 22.73, 25.83, 26.39, 29.49, 29.58, 29.92, 30.62, 32.03, 68.56, 73.55, 74.96, 106.79, 123.63, 130.71, 142.00, 150.34, 155.23. Elemental analysis: calculated for $C_{42}H_{77}KO_6S\cdot H_2O$ (%), C 65.67, H 10.38; found, C 66.36, H 10.49.

*Caesium 2,3,4-tris(dodecyloxy)benzenesulfonate (**8**).*

Compound **2** (0.71 g, 1.0 mmol) was dissolved in 50 ml ethanol at 60°C under a nitrogen atmosphere. Subsequently, 0.34 g (2.0 mmol) caesium hydroxide monohydrate was added and the reaction mixture was refluxed for 30 min. The solution was filtered hot and the filtrate was cooled down to room temperature. The resulting precipitate was isolated by filtration and washed several times with H_2O. After pre-drying in vacuum, the crude product was recrystallised twice from *n*-hexane to yield a white powder of **8**. Yield: 0.8 g>98%. M.p. 231.0°C (by DSC). TLC (6/1 $CHCl_3$/MeOH): R_f=0.44. ^{1}H NMR (300 MHz, $CDCl_3$, 20°C, TMS): δ 0.88 (t, 9H, CH_3, *J*=6.6 Hz), 1.26 (overlapped peaks, 48H, $CH_3(CH_2)_8$), 1.47 (broad, 6H, $O(CH_2)_2CH_2$), 1.72 (m, 6H, OCH_2CH_2), 3.90 (overlapped peaks, 6H, OCH_2, *J*=6.6 Hz), 7.03 (s, 2H, 2,6 position). ^{13}C NMR (75 MHz, $CDCl_3$, 20°C, TMS): δ 14.12, 22.71, 26.27, 29.44, 29.62, 29.80, 31.96, 31.96, 73.42, 106.7, 139.52, 140.03, 152.99. Elemental analysis: calculated $C_{42}H_{77}CsO_6S$ (wt %), C 59.84, H 9.21; found, C 59.71, H 9.23.

*Pyridinium 2,3,4-tris(dodecyloxy)benzenesulfonate (**9**).*

Compound **2** (0.50 g, 0.7 mmol) was dissolved in 10 ml pyridine under a nitrogen atmosphere. The solution was stirred at room temperature for 24 h and subsequently the pyridine was completely removed by evaporation under reduced pressure. The residue was twice recrystallised from methanol and finally dried in vacuum at 40°C to give white crystals of **9**. Yield: 0.5 g>98%. M.p. 81.2°C. TLC (6/1 $CHCl_3$/MeOH): R_f=0.65. ^{1}H NMR (300 MHz, $CDCl_3$, 20°C, TMS): δ 0.88 (t, 9H, CH_3, *J*=6.6 Hz), 1.27 (overlapped peaks, 48H, $CH_3(CH_2)_8$), 1.46 (overlapped peaks, 6H, $O(CH_2)_2CH_2$), 1.73 (m, 6H, OCH_2CH_2), 3.97 (overlapped t, 4H, 3- and 4-OCH_2), 4.18 (t, 2H, 2-OCH_2, *J*=6.98 Hz), 6.60 (d, 1H, 5-benzene-*H*, *J*=8.67 Hz), 7.70 (d, 1H, 6-benzene-*H*, *J*=8.67 Hz), 7.97 (t, 2H, 2,4 position in pyridium ring, *J*=6.99 Hz), 8.42 (t, 1H, 3 position in pyridium ring, *J*=7.73 Hz), 9.07 (d, 2H, 1,5 position in pyridium ring, *J*=5.31 Hz). ^{13}C NMR (75 MHz, $CDCl_3$, 20°C, TMS): δ 14.12, 22.69, 25.90, 26.11, 26.19, 29.27, 29.39, 29.70, 30.42, 31.94, 68.68, 73.66, 74.68, 106.61, 123.66, 126.96, 130.88, 142.26, 142.44, 145.27, 151.18, 155.54. Elemental analysis: calculated for $C_{47}H_{83}NO_6S$ (wt %), C 71.44, H 10.59, N 1.77; found, C 69.77, H 11.59, N 1.66.

*Tetramethylammonium 2,3,4-tris(dodecyloxy)benzenesulfonate (**10a**).*

Compound **2** (0.71 g, 1mmol) was dissolved in 50 ml ethanol under a nitrogen atmosphere. At 60°C, 0.8 ml (2.0 mmol) tetramethylammonium hydroxide (25 wt % in methanol) was added. The mixture was refluxed at 60°C for 30 min and filtered hot. The filtrate was stored at 4°C overnight. The resulting precipitate was isolated by filtration and washed twice with water. The crude product was twice recrystallised from *n*-hexane and subsequently dried in vacuum at 60°C to give white needle crystals of **10a**. Yield: 0.7 g, >98%. M.p. 89.8°C, TLC (6/1 $CHCl_3$/MeOH): R_f=0.12, ^{1}H NMR (300 MHz, $CDCl_3$, 20°C, TMS): δ 0.88 (t, 9H, CH_3, *J*=6.6 Hz), 1.27 (overlapped peaks, 48H, $CH_3(CH_2)_8$), 1.45 (m, 6H, $O(CH_2)_2CH_2$), 1.79 (m, 6H, OCH_2CH_2), 3.42 (s, 12H, $^+N(CH_3)_4$), 3.94 (t, 4H, 3- and 4-OCH_2, *J*=6.6 Hz), 4.16 (t, 2H, 2-OCH_2, *J*=7.17 Hz), 6.57 (d, 1H, 5-benzene-*H*, *J*=9.06 Hz), 7.57 (d, 1H, 6-benzene-*H*, *J*=9.06 Hz). ^{13}C NMR (75 MHz, $CDCl_3$, 20°C, TMS): δ 14.12, 22.69, 26.03, 26.14, 26.21, 29.40, 29.46, 29.66, 29.71, 29.77, 29.86, 31.94, 55.59, 68.63, 73.59, 74.50, 106.49, 123.21, 132.96, 142.34, 151.13, 154.86. IR (KBr, cm^{-1}): 3435.83 (s, broad), 2956.35 (m), 2920.78 (vs), 2875.95 (m), 2850.81 (s), 1630.32 (m, broad), 1583.60 (w), 1468.10 (m), 1436.11 (w), 1379.47 (w), 1300.63 (w), 1276.34 (w), 1216.62 (s), 1195.41 (m), 1156.99 (w), 1087.84 (s), 1063.19 (w), 1039.60 (w), 885.73 (w), 811.16 (w), 738.43 (w), 721.39 (w), 686.57 (w), 667.28 (w), 633.80 (w), 607.99 (w), 580.02 (w), 535.26 (w). Elemental analysis: calculated for $C_{46}H_{89}NO_6S$ (wt %), C 70.45, H 11.44, N 1.79; found, C 69.77, H 11.59, N 1.66.

*Tetraethylammonium 2,3,4-tris(dodecyloxy)benzenesulfonate (**10b**).*

Compound **2** (1.1 g, 1.5 mmol) was dissolved in 50 ml ethanol under a nitrogen atmosphere. At 60°C, 0.8 ml (2 mmol) tetraethylammonium hydroxide (25 wt % in methanol) was added. The mixture was stirred at 60°C for 30 min and filtered hot. The filtrate was stored at 4°C overnight. The precipitate was isolated by filtration and washed twice with water. The crude product was recrystallised twice from *n*-hexane and subsequently dried in vacuum at 60°C to give white crystals of **10b**. Yield: 1.2 g, >98%. M.p. 125.6°C. TLC (6/1 $CHCl_3$/MeOH): R_f=0.20. ^{1}H NMR (300 MHz, $CDCl_3$, 20°C, TMS): δ 0.90 (t, 9H, CH_3, J=6.71 Hz), 1.27 (overlapped peaks, 60H, $CH_3(CH_2)_8$ and $^+N(CH_2CH_3)_4$), 1.45 (m, 6H, $O(CH_2)_2CH_2$), 1.77 (m, 6H, OCH_2CH_2), 3.38 (tetra, 8H, $^+N(CH_2CH_3)_4$, J=7.17 Hz), 3.94 (tetra, 4H, 3- and 4-OCH_2, J=6.42 Hz), 4.17 (t, 2H, 2-OCH_2, J=7.16 Hz), 6.53 (d, 1H, 5-benzene-*H*, J=8.85 Hz), 7.61 (d, 1H, 6-benzene-*H*, J=8.67 Hz). ^{13}C NMR (75 MHz, $CDCl_3$, 20°C, TMS): δ 7.73, 14.14, 22.71, 26.09, 26.15, 26.22, 29.41, 29.72, 29.78, 30.46, 31.96, 52.60, 133.81, 142.30, 144.93, 145.27, 151.31, 154.46. IR (KBr, cm^{-1}): 3440.32 (s, broad), 2919.37 (vs), 2851.42 (vs), 1631.43 (w), 1583.89 (w), 1487.08 (m), 1468.70 (m), 1438.27 (m), 1379.08 (w), 1301.87 (w), 1277.64 (w), 1220.43 (m), 1194.21 (m), 1161.39 (w), 1129.02 (w), 1087.92 (m), 1064.11 (w), 1046.01 (w), 956.37 (w), 948.50 (w), 800.55 (w), 721.65 (w), 692.38 (w), 634.40 (w), 611.10 (w), 581.82 (w), 537.59 (w). Elemental analysis: calculated for $C_{50}H_{97}NO_6S$ (%), C 71.46, H 11.63, N 1.67; found, C 71.55, H 11.28, N 1.64.

*Tetrabutylammonium 2,3,4-tris(dodecyloxy)benzenesulfonate (**10c**).*

Compound **2** (1.1 g, 1.5 mmol) was dissolved in 50 ml ethanol under a nitrogen atmosphere. At 60°C, 0.8 ml (2.0 mmol) tetrabutylammonium hydroxide (25 wt % in methanol) was added. The mixture was refluxed at 60°C for 30 min and filtered hot. The filtrate was stored at 4°C overnight. The precipitate was filtered and washed twice with water. The crude product was recrystallised twice from *n*-hexane and subsequently dried in vacuum at 60°C to give white crystals of **10c**. Yield: 1.4 g, >98%. M.p. 85.1°C. TLC (6/1 $CHCl_3$/MeOH): R_f=0.46. ^{1}H NMR (300 MHz, $CDCl_3$, 20°C, TMS): δ 0.88 (m, 9H, CH_3), 0.96 (t, 12H, $(CH_3C_3H_6)_4N^+$, J=7.37 Hz), 1.27 (overlapped peaks, 48H, $CH_3(CH_2)_8$), 1.40 (m, 14H, $O(CH_2)_2CH_2$ and $(CH_3CH_2C_2H_4)_4N^+$), 1.63 (m, 8H, $(CH_3CH_2CH_2CH_2)_4N^+$), 1.83 (m, 6H, OCH_2CH_2), 3.31 (t, 8H, $^+N(CH_2C_2H_4CH_3)_4$, J=8.12 Hz), 3.94 (overlapped t, 4H, 3- and 4-OCH_2), 4.18 (t, 2H, 2-OCH_2, J=7.16 Hz), 6.51 (d, 1H, 5-benzene-*H*, J=8.67 Hz), 7.63 (d, 1H, 6-benzene-*H*, J=8.67 Hz). ^{13}C NMR (75 MHz, $CDCl_3$, 20°C, TMS): δ 13.70, 14.12, 19.70, 22.69, 24.09, 26.08, 26.12, 26.21, 29.39, 29.46, 29.65, 29.69, 29.76, 30.44, 30.53, 31.94, 58.71, 68.56, 74.48, 106.19, 134.17, 142.29, 151.41, 154.29. IR (KBr, cm^{-1}): 3437.84 (s, broad), 2918.15 (vs), 2582.00 (s), 1633.53 (m), 1583.19 (m), 1467.97 (m), 1438.32 (m), 1375.90 (w), 1303.52 (w), 1276.11 (w), 1211.57 (s), 1156.19 (w), 1085.04 (m), 1041.41 (w), 801.63 (w), 721.46 (w), 684.15 (w), 610.77 (w), 578.15 (w), 536.00 (w). Elemental analysis: calculated for $C_{58}H_{113}NO_6S$ (%), C 73.13, H 11.96, N 1.56; found, C 72.40, H 11.05, N 1.47.

*3,4,5-Trihydroxybenzenesulfonic acid (**11**).*

Through 100 ml of an aqueous solution of pyrogallol (10 g, 0.08 mol), Na_2SO_3 (24.1 g, 0.19 mol) and NaOH (3.34 g, 0.08 mol) air was blown over a period of 5 h. The reaction solution was acidified with 40 ml HCl solution (16%) and was continuously extracted with diethyl ether for 48 h in a liquid/liquid separator. From this pre-purified aqueous solution, all SO_3^{2-} ions were removed by adding barium acetate solution (48.84 g, 0.191 mol). Subsequently, the filtrate was run over an ion-exchange column (Amberlite IR120) to remove remaining metal ions. After that treatment the solution was decolourised by boiling with 1 g of activated charcoal for 15 min. Upon evaporation of water under vacuum white crystals separated. The crude product was dried over P_4O_{10} under vacuum for 24 h to produce 9.98 g of **11**. Yield: 9.98 g, ≅61%. M.p. 39–40°C. ^{1}H NMR (300 MHz, D_2O, 20°C): δ 6.95 (s, 2H, aromatic *H*). ^{13}C NMR (75 MHz, D_2O, 20°C): δ 105.89 (2-benzene-*C*), 133.91 (4-benzene-*C*), 135.42 (1-benzene-*C*), 144.80 (3-benzene-*C*).

*Lithium 2,3,4-tris(dodecyloxy)benzenesulfonate (**12**).*

3,4,5-Trihydroxybenzenesulfonic acid (3.0 g, 4.22 mmol) and Li_2CO_3 (10.75 g, 149 mmol) were mixed with 50 ml of dried DMF under nitrogen atmosphere. At 100°C, 6.3 ml (26 mmol) of 1-bromododecane were added dropwise. The reaction mixture was stirred for 48 h at 100°C and subsequently slowly poured into 50 ml of ice water. After washing the aqueous phase for three times with chloroform, acetone was added to the aqueous solution until no further precipitation occurred. The precipitate was isolated by filtration and recrystallised twice from each 100 ml of methanol to give a crude light yellow

powder. The final purification was performed by column chromatography over silica gel with a mobile phase composed of methanol and $CHCl_3$ (1/6, vol/vol) to yield **12** as a white solid. Yield: 50 mg=1.65%. M.p. 53.7°C (by DSC). TLC (6/1 $CHCl_3$/MeOH): R_f=0.31. ^{1}H NMR (300 MHz, DMSO-d_6, 20°C, TMS): δ 0.86 (t, 9H, CH_3, J=6.8 Hz), 1.25 (overlapped peaks, 54H, $CH_3(CH_2)_9$), 1.62 (m, 6H, OCH_2CH_2), 3.20 (m, 4H, 3- and 5-OCH_2), 3.83 (t, 2H, 4-OCH_2, J=6.8 Hz), 6.59 (s, 2H, 2,6-benzene-*H*). ^{13}C NMR (75 MHz, DMSO-d_6, 20°C, TMS): δ=13.86 (CH_3), 21.53 (CH_3CH_2), 22.02 ($OCH_2CH_2CH_2$), 29.36 ($CH_3CH_2CH_2CH_2$), 29.01 ($CH_3CH_2CH_2CH_2(CH_2)_5$, 29.38 (OCH_2CH_2), 31.22 ($CH_3CH_2CH_2$), 71.56 (OCH_2), 105.08 (2,6-benzene-*C*), 134.30 (4-benzene-*C*), 143.27 (1-benzene-*C*), 149.70 (3,5-benzene-*C*).

*Sodium 3,4,5-tris(dodecyloxy)benzenesulfonate (**13**).*

3,4,5-Trihydroxybenzenesulfonic acid (1.0 g, 1.4 mmol) and 6.76 g (63.8 mmol) Na_2CO_3 were mixed with 50 ml of dried DMF under nitrogen atmosphere. At 100°C, 3.5 ml (14.6 mmol) of 1-bromododecane were added dropwise. The reaction mixture was stirred for 48 h at 100°C and subsequently slowly poured into 50 ml of ice water. After washing the aqueous phase three times with chloroform, acetone was added to the aqueous solution until no further precipitation occurred. The precipitate was isolated by filtration and recrystallised twice from 100 ml of methanol to give a crude light yellow powder. The final purification was performed by column chromatography over silica gel with a mobile phase composed of methanol and $CHCl_3$ (1/6, vol/vol) to yield **13** as a white solid. Yield: 450 mg, 43.9%. M.p. −7.1°C (by DSC). TLC (6/1 $CHCl_3$/methanol): R_f=0.59. ^{1}H NMR (300 MHz, $CDCl_3$, 20°C, TMS): δ 0.88 (t, 9H, CH_3, J=6.6 Hz), 1.26 (overlapped peaks, 48H, $(CH_2)_8$), 1.47 (broad, 6H, $O(CH_2)_2CH_2$), 1.72 (m, 6H, OCH_2CH_2), 3.90 (overlapped peaks, 6H, OCH_2, J=6.6 Hz), 7.03 (s, 2H, 2,6-benzene-*H*). ^{13}C NMR (75 MHz, $CDCl_3$, 20°C, TMS): δ 14.12, 22.71, 26.27, 29.44, 29.62, 29.80, 31.96, 31.96, 73.42, 106.7, 139.52, 140.03, 152.99.

*Potassium 3,4,5-tris(dodecyloxy)benzenesulfonate (**14**).*

3,4,5-Trihydroxybenzenesulfonic acid (1.0 g, 1.4 mmol) and 6.76 g (49.0 mmol) K_2CO_3 were mixed with 50 ml of dried DMF under nitrogen atmosphere. At 100°C, 3.5 ml (14.6 mmol) of 1-bromododecane were added dropwise. The reaction mixture was stirred for 48 h at 100°C and subsequently slowly poured into 50 ml of ice water. After washing the aqueous phase three times with chloroform, acetone was added to the aqueous solution until no further precipitation occurred. The precipitate was isolated by filtration and recrystallised twice from 100 ml of methanol to give a crude light yellow powder. The final purification was performed by column chromatography over silica gel with a mobile phase composed of methanol and $CHCl_3$ (1/6, vol/vol) to yield **14** as a white solid. Yield: 0.45 g≅43.0%. M.p. 231.0°C. TLC (6/1 ethyl acetate/methanol): R_f=0.15. ^{1}H NMR (300 MHz, $CDCl_3$, 20°C, TMS): δ 0.88 (t, 9H, CH_3, J=6.6 Hz), 1.26 (overlapped peaks, 48H, $(CH_2)_8$), 1.47 (broad, 6H, $O(CH_2)_2CH_2$), 1.72 (m, 6H, OCH_2CH_2), 3.90 (overlapped peaks, 6H, OCH_2, J=6.6 Hz), 7.03 (s, 2H, 2,6-benzene-*H*). ^{13}C NMR (75 MHz, $CDCl_3$, 20°C, TMS): δ=14.12, 22.71, 26.27, 29.44, 29.62, 29.80, 31.96, 31.96, 73.42, 106.7, 139.52, 140.03, 152.99.

*Caesium 2,3,4-tris(dodecyloxy)benzenesulfonate (**15**).*

3,4,5-Trihydroxybenzenesulfonic acid (5.0 g, 7.03 mmol) and 23.8 g (73.05 mmol) Cs_2CO_3 were mixed with 60 ml of dried DMF under nitrogen atmosphere. At 100°C, 10 ml (41.6 mmol) of 1-bromododecane were added dropwise. The reaction mixture was stirred for 48 h at 100°C and subsequently slowly poured into 50 ml of ice water. The precipitate was isolated by filtration and recrystallised twice from 100 ml of methanol to give a white powder of **15**. Yield: 1800 mg, 30.4%. M.p. 116.9°C (by DSC). TLC (6/1 $CHCl_3$/methanol): R_f=0.46, ^{1}H NMR (300 MHz, $CDCl_3$, 20°C, TMS): δ 0.88 (t, 9H, CH_3, J=6.6 Hz), 1.26 (overlapped peaks, 48H, $CH_3(CH_2)_8$), 1.43 (broad, 6H, $OCH_2(CH_2)_2$), 1.72 (m, 6H, OCH_2CH_2), 3.90 (m, 6H, OCH_2, J=6.6 Hz), 7.03 (s, 2H, 2,6-benzene-*H*). ^{13}C NMR (75MHz, $CDCl_3$, 20°C, TMS): δ=14.12, 22.71, 26.27, 29.44, 29.62, 29.80, 31.96, 31.96, 73.42, 106.7, 139.52, 140.03, 152.99. Elemental analysis: calculated (%), C 59.84, H 9.21; found, C 59.06, H 9.30.

3. Results and discussion

Syntheses

2,3,4-Tris(alkoxy)benzenesulfonates are readily accessible by sulfonation of 2,3,4-tris(alkoxy)benzenes prepared by alkylation of pyrogallol (1,2,3-trihydroxybenzene), as depicted in Scheme 1. 1,2,3-Trihydroxybenzene was alkylated with 1-bromododecane in DMF to produce 1,2,3-tris(dodecyloxy)-benzene (**1**) in 76% yield after recrystallisation from acetone (*19*).

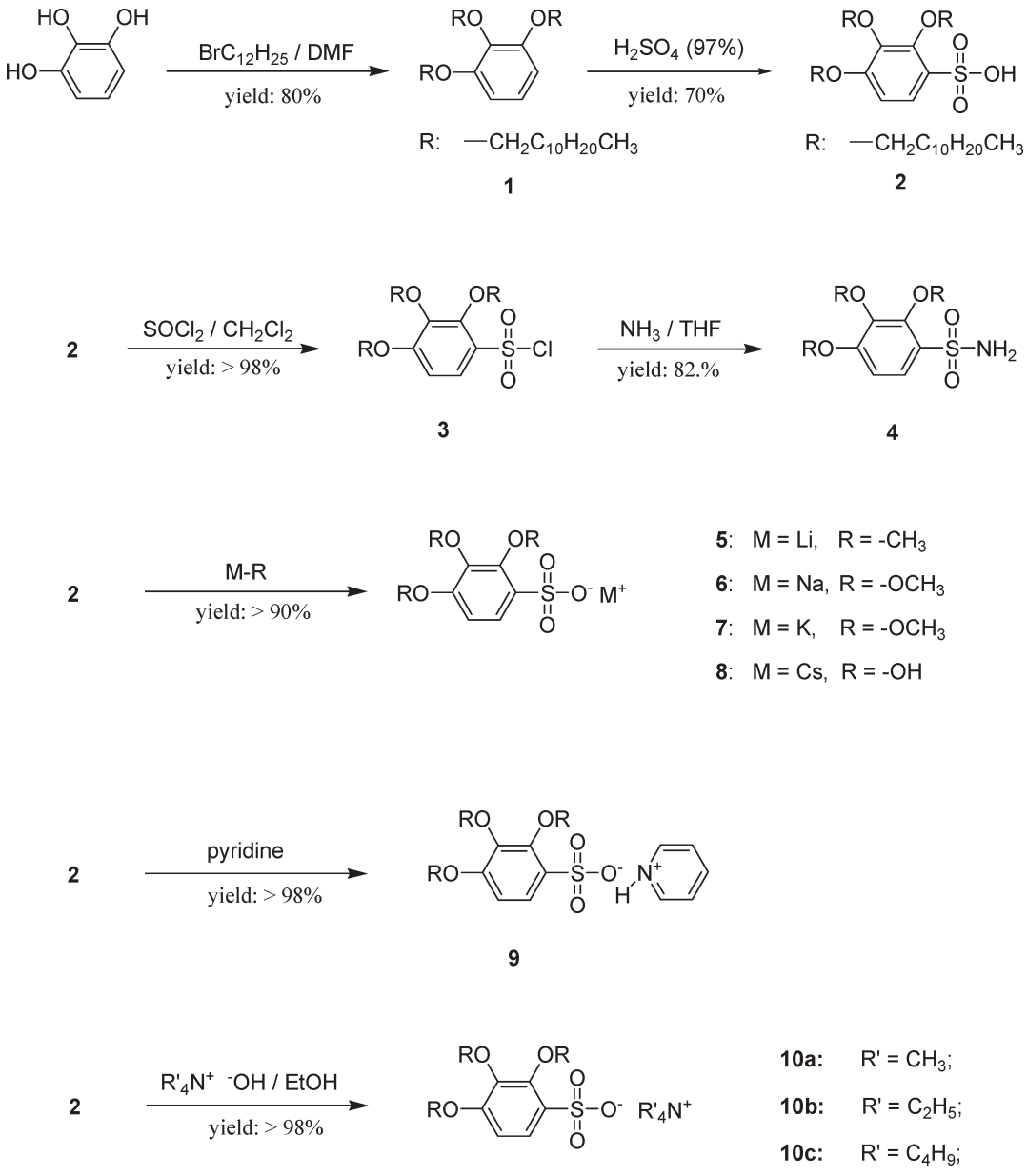

Scheme 1. Synthesis of 2,3,4-tris(dodecyloxy)benzenesulfonic acid and its derivatives.

Sulfonation of the 1,2,3-tris(dodecyloxy)benzene was carried out with concentrated sulfuric acid at 20°C for 2 h to produce 2,3,4-tris(dodecyloxy)benzenesulfonic acid (**2**) in 88.7% yield after recrystallisation from *n*-hexane. Lithium (**5**), sodium (**6**), potassium (**7**) and caesium sulfonates (**8**) were synthesised by neutralising the sulfonic acid **2** with methyllithium, sodium methoxide, potassium methoxide and caesium hydroxide, respectively, at room temperature. The pyridinium sulfonate (**9**) and the alkylammonium sulfonates (**10a**–**10c**) were produced analogously by converting **2** with the corresponding organic nitrogen bases at room temperature to obtain the products in nearly quantitative yield. Reacting the sulfonic acid **2** with thionyl chloride yielded sulfonyl chloride **3** that could be transformed into 2,3,4-tris(dodecyloxy)-benzenesulfonamide **4** by dissolving compound **3** in ammonia gas saturated THF, and storing the mixture for one week at 30°C.

Attempts were made to produce 2,3,4-tris(alkoxy)benzenesulfonic acids with shorter alkoxy chains (pentyloxy–decyloxy). The reactions yielded oily products that could not be purified by crystallisation because of their low melting temperatures. Column chromatography on silica gel was unsuccessful too, since the highly polar molecules permanently adhered to the stationary phase. The

description of their preparation and purification via suitable salts will be the matter of a subsequent publication.

Based on the mechanism of electrophilic substitution the sulfonation of 1,2,3-alkoxybenzenes will always occur in position 4 or 6 of the benzene ring, hence the symmetrically substituted 3,4,5-derivatives cannot be prepared by this method. It is known that nitration in 5-position of the 1,2,3-alkoxybenzene ring can be achieved on reacting the aromatic with silica-adsorbed nitric acid (*20*). However, the analogous reaction with silica-adsorbed sulfuric acid failed to yield the symmetrically substituted product.

three steps. First, organic impurities were washed off by continuous extraction of the reaction mixture with diethyl ether, subsequently all sulfite ions were removed by precipitation with barium acetate, and finally the organic acid was liberated by cation exchange. After adsorption of remaining yellow-brownish colorants on activated charcoal, the acid was isolated from the aqueous solution and dried over phosphorus pentoxide *in vacuo* to yield 61% of pure acid **11**.

Compounds **12**–**15** were synthesised from **11** by alkylation with 1-bromododecane in dry DMF using the corresponding alkali metal carbonates (M_2CO_3:

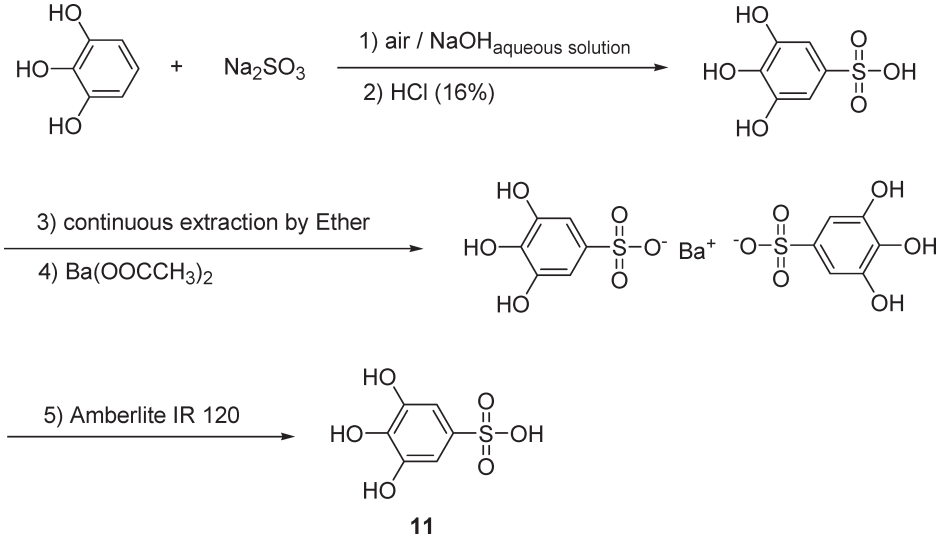

11

Scheme 2. Synthesis of 3,4,5-trihydroxybenzenesulfonic acid (**11**).

The synthesis of the desired products was performed via the preparation of 3,4,5-trihydroxybenzenesulfonic acid. The preparation of this compound has been described previously by sulfonation of pyrogallol with concentrated sulfuric acid (*21*). However, since mixtures of isomers were obtained, it was decided to generate the sulfonic acid under oxidative sulfonation conditions, as depicted in Scheme 2. Pyrogallol was oxidised in an alkaline solution of sodium sulfite with air. Since phenols rapidly form black oxidation products in the presence of bases and oxygen, the obtained crude 3,4,5-trihydroxybenzenesulfonic acid had to be purified in

M=Li, Na, K, Cs) as base (see Scheme 3). The purification of **12**–**14** (Li, Na, K) was achieved by column chromatography over silica on elution with mixtures from methanol and chloroform.

The caesium sulfonate **15** could simply be purified by recrystallisation from hot methanol and subsequent freeze-drying from benzene. The purity of the synthesised materials was checked by ^{1}H NMR, and TLC to exceed 95% in all cases. Elemental analyses performed without pre-drying of the samples were consistent with either the dry salt or its monohydrate. The salts were freeze dried and stored under dry nitrogen prior to use for thermal characterisation.

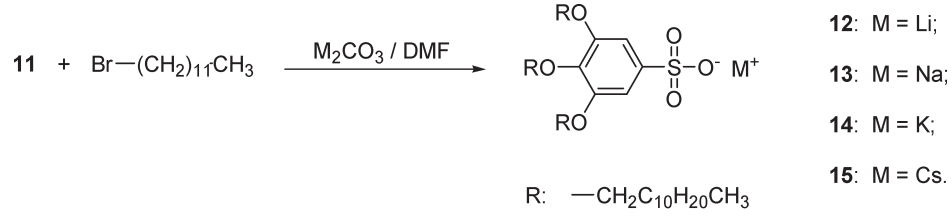

12: M = Li;
13: M = Na;
14: M = K;
15: M = Cs.

Scheme 3. Synthesis of (a) 3,4,5-tris(dodecyloxy)benzenesulfonates **12**–**15** by alkylation of 3,4,5-trishydroxybenzenesulfonic acid **11**.

Thermal analysis

Thermal characterisation was carried out by a combination of DSC and hot-stage thermo-optical polarised microscopy (TOPM). Transition temperatures were determined by DSC at a heating/cooling rate of 10°C min^{-1}. The DSC measurement programme consisted of several subsequent heating and cooling runs to detect the occurrence of 'virgin phases'. The discussion below is based on the transitions observed during the second heating scans, as compiled in Table 1–2. The assignment of the type of thermal transition was supported by microscopic observations. Table 1 summarises the measured transition temperatures as well as the corresponding enthalpy changes of compounds **2**–**10**, whereas Table 2 contains the respective thermal analysis data on the symmetrically substituted sulfonates **12**–**16**.

The prepared amphiphilic sulfonate derivatives can be divided into hydrogen bonded and ionic compounds. Only two representatives of the first class, i.e. acid **2** and sulfonamide **4**, have been prepared. Whereas the sulfonic acid is a crystalline material, melting at 55.7°C to an isotropic phase, the sulfonamide **4** exhibits a columnar mesophase between 55 and 118°C (see Figure 1). This is a first important difference to the analogous 2,3,4-tris(dodecyloxy) benzamides, which do not form mesophases because the presence of an alkoxy chain in the 2-position of a carboxylic acid amide impedes the formation of a hydrogen bonded network due to steric hindrance (*8, 22*).

Figure 2 (a) shows the DSC thermogram of the asymmetrically substituted lithium salt **5**, which is also qualitatively representative for the sodium salt **6**. The first heating was characterised by three endothermic signals at 93, 118, 161°C and 53, 103.5, 145°C, respectively.

Table 1. Phase transition temperatures (°C) and enthalpies (kJ mol^{-1}, in parentheses) of the 2,3,4-tris(dodecyloxy)benzenesulfonate compounds **2**–**10** as obtained from DSC measurements (on second heating at 10 K min^{-1}).

No.		Phase sequence
2	–OH	Cr 56 (32.6) I
4	$-NH_2$	Cr 55 (37.4) Col_{hd} 118 (3.9) I
5	LI^+	Cr –11 (6.7) Cub 161 (0.3) I
6	Na^+	Cr –3 (10.1) Cub_{Im3} 103 (3.5) I
7	K^+	Cr 18 (21.5) M_1 47 (1.4) M_2 124 (5.9) Col_{hd} 171 (3.1) I
8	Cs^+	Cr 50 (23.5) Col_{hd} 193 (2.2) I
9	Py^+	Cr 30 (−25.1) Cr_2 53 (−5.1) Cr_3 80 (71.5) Col_{hd} 122 (1.1) I
10a	Me_4N^+	Cr 47 (20.5) M_1 130 (5.9) M_2 154 (9.2) M_3 231 (1.3) I
10b	Et_4N^+	Cr 125 (77.0) {98.5 M_{mono}} I
10c	Bu_4N^+	Cr 81 (74.5) I

Cr=crystalline phase, Cub=cubic mesophase, Col_{hd}=hexagonal disordered columnar mesophase, M=mesophase type not determIined, {M_{mono}}=monotropIc mesophase, I=isotropic liquid.

Table 2. Phase transition temperatures (°C) and enthalpies (kJ mol^{-1}, in parentheses) of the 3,4,5-tris(dodecyloxy)benzenesulfonates **12**–**15** as obtained from DSC measurements (on second heating at 10 K min^{-1}).

No.		Phase sequence
12	Li^+	Cr 52 (7.8) M_1 148 (7.1) M_2>250 dec
13	Na^+	Cr 5 (6.8) M_1 143 (25.3) M_2>250 dec
14	K^+	Cr –9 (12.6) M_1 173 (2.3) M_2>250 dec
15	Cs^+	Cr –3 (13.9) Col_{ho} 50 (2.2) Col_{hd} 144 (2.3) Cub 190 (0.2) I

Cr=crystalline phase, Cub=cubic mesophase, Col_{ho}=hexagonal ordered columnar mesophase, Col_{hd}=hexagonal disordered columnar mesophase, M=mesophase type not determined, dec=decomposition, I=isotropic liquid.

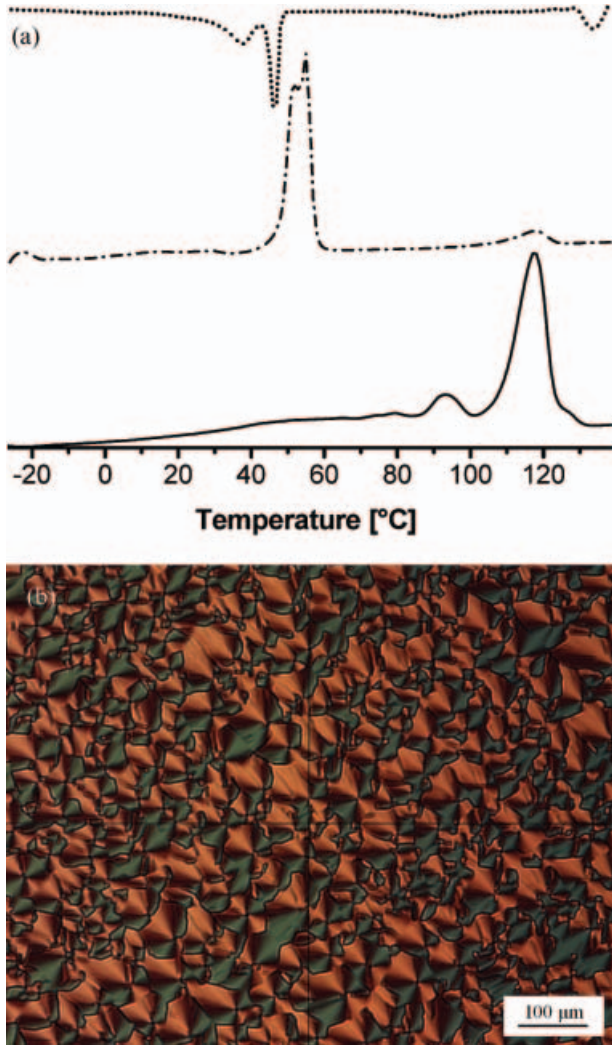

Figure 1. (a) DSC thermogram of sulfonamide **4** (— first heating, ·—·— second heating, ... cooling) and (b) texture of **4** between crossed polarisers at 80°C.

Both salts form highly viscous, but optically isotropic liquids above the respective highest DSC melting endotherm. During the first heating, the melt viscosity of both the compounds reduced abruptly on increasing the temperature above the second endotherm (**5**: $T=161^{\circ}C$, **6**: $T=145^{\circ}C$). Since the high viscous phase did not show shear-induced birefringence, the presence of a cubic mesophase was deduced for both salts.

However, the detailed phase behaviour of compounds **5** and **6** proved to be different. The small-angle X-Ray scattering (SAXS) pattern of the lithium salt **5** consisted of nine reflections at room temperature (Figure 3, curve (a)). Five reflections with ratios of the squares of the corresponding *d*-spacings equal to 1:3:4:7:9, can be attributed to the two-dimensional (2D) hexagonal lattice with a column diameter of $a=4.6\,nm$ ($d_{10}=3.95\,nm$). Three other reflections exhibited *d*-spacings of 3.5 nm, 1.75 nm and 1.17 nm, and originated from ordering along the column axes. This assumption is supported by the observation of a reflection with index 101. It is important to note that all the observed reflections are equally narrow. On the basis of these facts, we can confidently claim the formation of a 3D hexagonal phase in the lithium salt **5** at room temperature. Unfortunately we could not obtain substantially oriented fibre to support our interpretation of the powder SAXS pattern.

Upon heating, the 00*l* maxima did not change their position, but gradually lost intensity, and eventually vanished at 100°C (Figure 3, curves (b)–(c)). Simultaneously the intensities of the equatorial reflections virtually did not change, whereas the *d*-spacings corresponding to the 2D hexagonal order decreased in correspondence to a thermal expansion coefficient $\beta=-4\times10^{-4}\,K^{-1}$. Thus, the first phase transition in the as-received compound **5** corresponds to the loss of the intracolumnar order, though we did not observe a jump in the column diameter, which was found to be characteristic of the order–disorder transition in columnar phases with their mesogenic groups tilted to the cylinder axis (*23*).

The second transition at 118°C was accompanied by the drastic change of small-angle scattering. Large grain structures developed, giving rise to a number of very sharp reflections (Figure 4, compare curves (b) and (c)). These peaks are caused by the slit collimation of Kratky camera, and correspond to the same reflection, caused by the grains located at

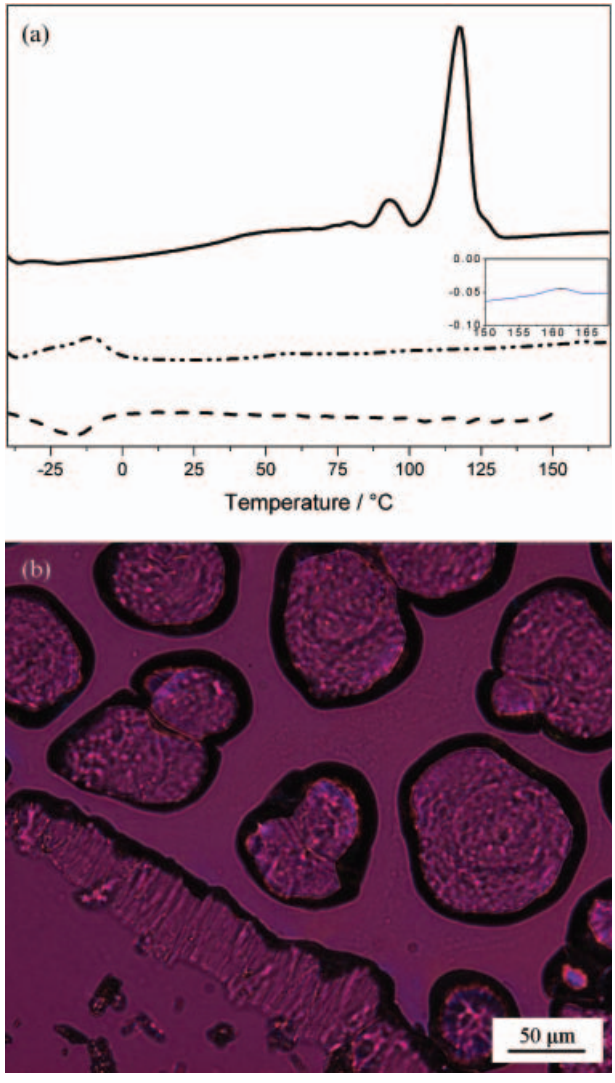

Figure 2. (a) DSC thermogram of lithium salt **5** (— first heating, −·−·− second heating, ... cooling) and (b) texture of **5** between crossed polarisers at 30°C.

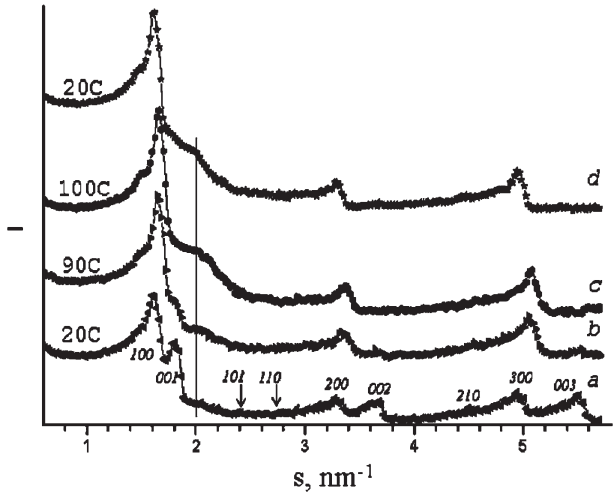

Figure 3. SAXS patterns of lithium 2,3,4-tris(dodecyloxy) benzenesulfonate **5**: (a) 'as-received' at 20°C; heated up to (b) 90°C; (c) 100°C; (d) successive cooling down to room temperature. Tail parts multiplied by 5 and shifted to previous positions for all plots.

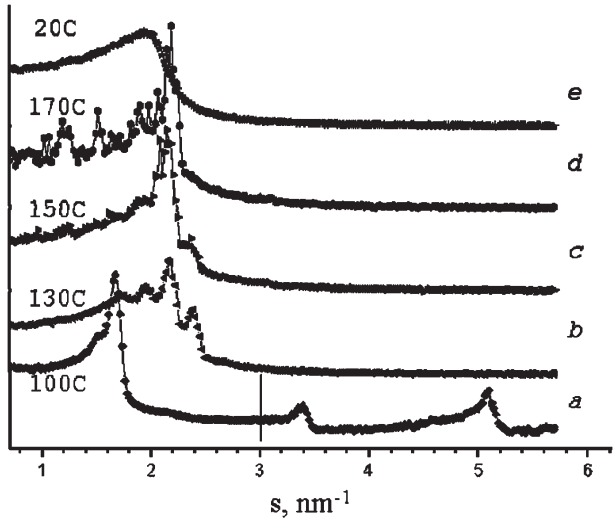

Figure 4. SAXS patterns of lithium 2,3,4-tris(dodecyloxy)-benzenesulfonate **5**: (a–c) heated up to 100°C, 130°C, 150°C, respectively; (d) grain structure developed at 170°C; (e) cooled down to room temperature after 170°C. Tail parts multiplied by 5 and shifted to previous positions for (a).

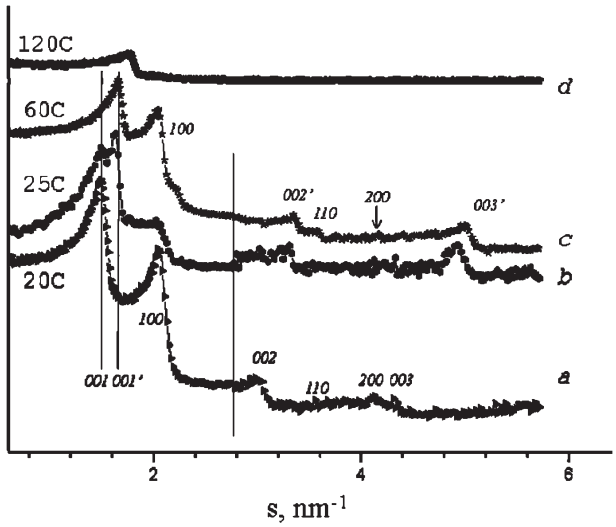

Figure 5. SAXS patterns of sodium 2,3,4-tris(dodecyloxy)benzenesulfonate **6**: (a) as-received at 20°C, (b, c) heated up to 25 and 60°C, respectively; (d) above the isotropisation temperature at 120°C. Tail parts multiplied by 5 and shifted to previous positions for (a), (b) and (c).

different azimuthal positions. The slit collimation leads to an apparent shift of the observed position of reflections, which are far apart from the equator. The development of this highly grained structure was confirmed by 2D X-ray patterns that are characteristic for cubic phases. We can also refer to the TOPM data, showing the presence of highly viscous and optically isotropic substance above the second DSC endotherm. The melt viscosity falls abruptly at 161°C due to the isotropisation of the sample. Transition to the cubic mesophase is irreversible (or, at least, kinetically hindered); we did not observe the development of hexagonal phase in samples upon cooling.

The SAXS pattern of the as-received sodium salt **6** (Figure 5 (a)) was similar to that of compound **5**: seven reflections can be easily divided into two subsets with the ratios of *d*-spacing squares 1:3:4:7 and 1:4:9 (first, second and third orders), which is indicative for the formation of a 3D hexagonal phase with cylinder diameter of a_h=3.6 nm and the fibre repeat equal to d_{001}=4.2 nm. On heating up to 60°C, three new reflections with *d*-spacing ratio 1:2:3 and $d_{001}{}^{*}$=3.8 nm appeared and gradually gained in intensity, whereas the set of meridional reflections with d_{001}=4.2 nm eventually disappeared (Figures 5 (b)–5 (c)). This can be explained by an order–order intracolumnar transition, corresponding to the first endotherm of DSC trace of the as-received sample. It is interesting to note that the heat of fusion of the order–order transition in compound **6** is about 2.5 times higher than that of the order–disorder transition in Li salt **5** (19.4 *vs.* 8.0 kJ mol^{-1}). This can be an indication of strong differences in the organisation of the mesogen groups in those two materials. Another argument for the same conclusion comes from the comparison of column diameters at room temperature: 4.6 nm in lithium salt *vs.* 3.6 nm in the sodium compound.

At further heating above 110°C (Figure 5 (d)) a wide lone reflection, corresponding to *d*=3.3nm, developed. No grain structure has been observed. However, on the basis of TOPM data similar to those for the cubic phase in **5**, we can conclude that a plastic crystal of cubic symmetry formed at ~100°C and melted at 145°C.

After cooling the sample, it underwent an irreversible transition to a cubic phase with lattice parameter *a*=7.1 nm at room temperature (Figure 6 (a)). The ratio of *d*-spacing squares was 2:4:8:10:16:22 with weak traces of reflections attributed to $d_1{}^2$:$d_7{}^2$:$d_8{}^2$=2:12:14. This pattern is characteristic for the symmetry class *Im*3. The further second heating shifted the maxima of the cubic phase to wider angles (*d*-spacing increased) and the peaks become more diffuse, lost intensity and disappeared completely at temperature above 120°C (Figures 6 (b)–6 (c)). Upon cooling to room temperature, the cubic phase was restored, although the reflections were still rather diffuse. It should be noted that the recovery occurred only in air (Figure 6 (d)).

The potassium salt **7** showed a complex phase sequence involving three subsequent liquid crystalline phases (Figure 7 (a)). Although DSC clearly revealed four phase transitions between 0°C and 180°C, only

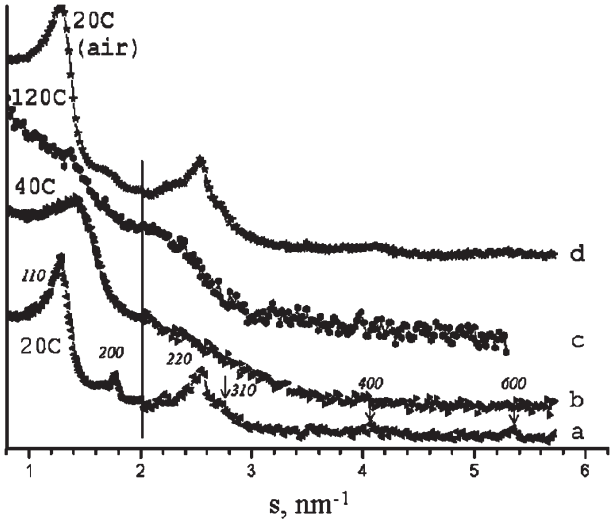

Figure 6. SAXS patterns of sodium 2,3,4-tris(dodecyloxy)-benzenesulfonate **6**: (a) cubic phase observed after cooling to room temperature; (b) heated up to 40°C; (c) transition to melt at 120°C with subsequent cooling (d). Tail parts multiplied by 5 and shifted to previous positions for all plots.

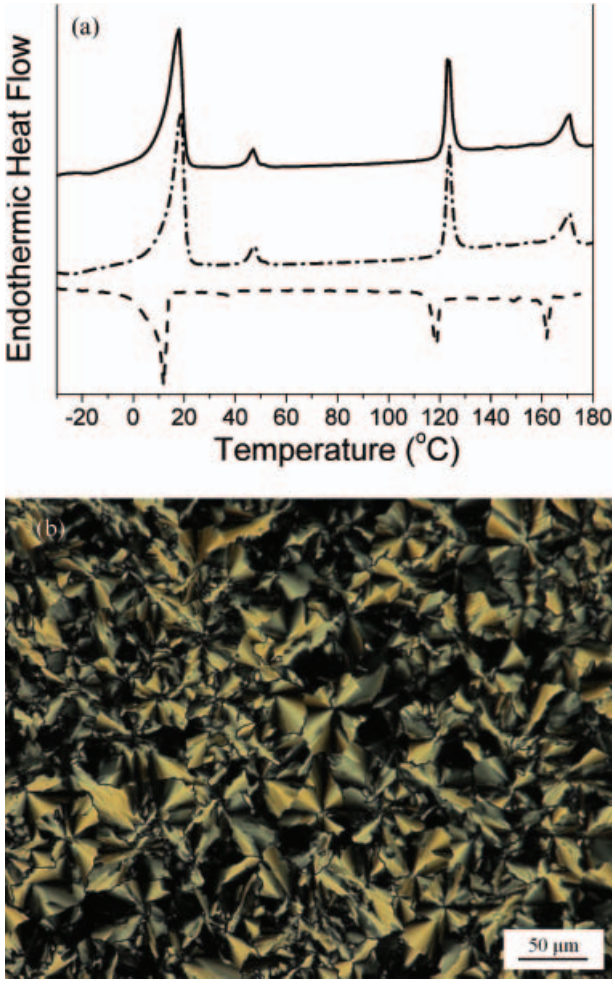

Figure 7. (a) DSC thermograms of potassium salt **7** (— first heating, −·−·− second heating, ... cooling) and (b) texture of **7** between crossed polarisers at 120°C.

one single type of optical texture was observed under polarised light. The fan-like texture formed on cooling below the clearing temperature of 171°C and did not significantly change on cooling to ambient temperature. However, without supporting X-ray structure determination it should not be speculated on a possible structural similarity of the three phases.

The caesium sulfonate **8** and pyridinium sulfonate **9** both exhibited a mesophase that showed optical textures characteristic of columnar phases. Whereas the caesium salt was stable at elevated temperatures ($T>240$°C) for several minutes, the pyridinium salt lost its optical anisotropy even after short heating to 150°C, accompanied by the evolution of gaseous decomposition products.

Figure 8 shows the SAXS patterns of caesium 2,3,4-tris(dodecyloxy)benzenesulfonate (**8**) at different temperatures. Prior to the first heating ("as-prepared state") the compound was characterised by a number of narrow reflections, which were indexed by means of a monoclinic lattice with parameters $a=6.58$ nm, $b=2.88$ nm, $c=1.27$ nm, and $\beta=102°$. It should be noted that the most intense reflections have $hk0$ indices. At ~50°C, the SAXS pattern changed sharply, showing at least four reflections with d-spacing ratios of $d_1^2:d_2^2:d_3^2:d_4^2=1:3:4:7$, which is highly indicative of a hexagonal columnar phase.

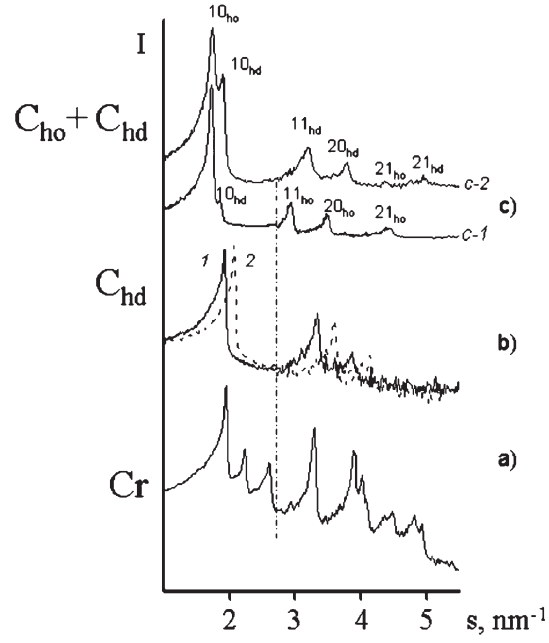

Figure 8. SAXS patterns of caesium 2,3,4-tris(dodecyloxy)-benzenesulfonate **8**: (a) as-received at 20°C; (b) heated up to 70°C (——) and 120°C (---); (c) room temperature after cooling from 70°C with different ratio of ordered and disordered columnar phases: (1) mostly C_{ho}, (2) C_{hd} prevails. Tail parts are multiplied by a factor of 5 and shifted.

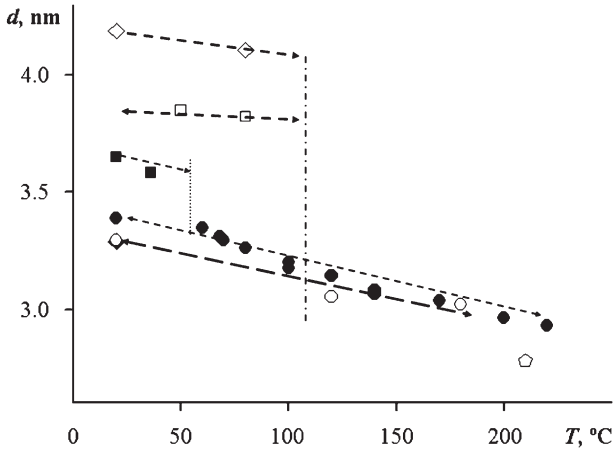

Figure 9. Temperature dependence of *d*-spacing of the first reflection for caesium sulfonate **8** (solid symbols) and **15** (hollow symbols). Squares: d_{10} of C_{ho} phase; circles: d_{10} of C_{hd} phase; diamonds: virgin phases; pentagon: cubic phase. Vertical lines correspond to order–disorder transition.

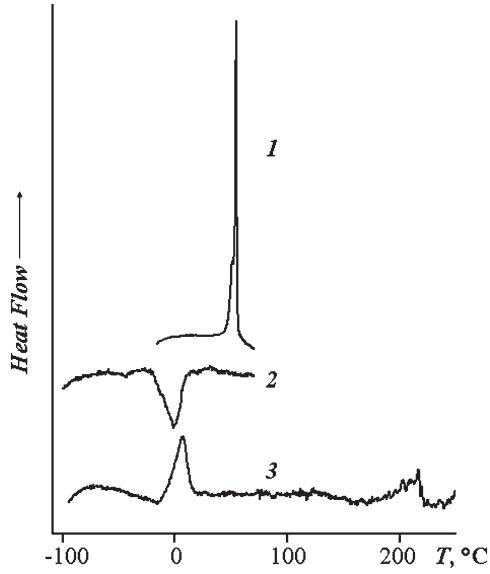

Figure 10. DSC scans of caesium 2,3,4-tris(dodecyloxy)-benzenesulfonate **8**: (1) first heating, multiplied by a factor of 1/20; (2) cooling; (3) second heating.

The cylinder diameter was 3.8 nm and decreased with increasing temperature, exhibiting a negative thermal expansion coefficient of $\beta = -(7.5 \pm 1) \times 10^{-4}\,K^{-1}$ until isotropisation at ~220°C. As shown in Figure 9, the columnar diameter became 3.4 nm at this temperature.

Note that negative thermal expansion coefficients, observed for alkali salts **5**–**8**, are quite widespread for columnar mesophases (*24, 25*). The decrease of column diameters has been attributed to the softening of the columns outer rim, which allows for a more dense packing of the column centres and to the shrinking of the aliphatic chains because of the occurrence of an increasing number of gauche-conformers with growing temperature (*26*). The intensity of the reflections did not change over the whole existence range of the columnar phase, but rapidly declined near the isotropisation temperature. Since the heat of isotropisation was rather low ($2.2\,kJ\,mol^{-1}$) it was concluded that the hexagonal columnar phase of compound **8** at $T > 70$°C was of the disordered type (Col_{hd}) and no internal order in the mutual positions of the wedge-like units exists. This conclusion is supported by wide-angle X-ray pattern, which gave no crystal reflections.

Upon cooling to room temperature, four new reflections (Figure 8 (c)) attributed to the columnar phase with a cylinder diameter of 4.2 nm appeared, whereas the reflections corresponding to the disordered columnar phase still remained. Relative intensities of these phases were very sensitive to ambient temperature.

This observation can be understood by comparing the DSC traces of the first and second heating runs (Figure 10). During the first heating, the crystalline phase melted at 55°C (heat of fusion: $58.1\,kJ\,mol^{-1}$); however, the further sequence of heating and cooling runs revealed that a *reversible* transition occured with a temperature maximum at 7°C on heating ($\Delta H = 11.6\,kJ\,mol^{-1}$). The heat of transition (*27*), as well as the observed characteristic jump of the cylinder diameter from 4.2 nm to 3.9 nm, indicated the presence of an order–disorder transition in the columns. As the transition temperature range is rather broad (from −10°C to 25°C), the two phases coexist at room temperature and cause the two sets of reflections depicted in Figure 8 (c). The role of air in the recovery of ordered phase should also be taken into account.

Preliminary results of molecular modelling of compound **8** gave the diameter of the column equal to 4.8 nm, when all the alkyl tails are in *trans*-conformation, which is in a good agreement with the model proposed.

Compound **9** became optically isotropic on prolonged annealing in its mesophase at 110°C without observable decomposition. The resulting material proved to be neither homeotropically oriented calamitic nor a columnar mesophase and on subsequent heating/cooling cycles it did not show any phase transition. If the compound was not overheated it exhibits a reversible transition from a columnar disordered phase into an ordered columnar upon slow heating and cooling cycles.

The polarised optical textures in the liquid crystal phase and the specific type of defects formed by the

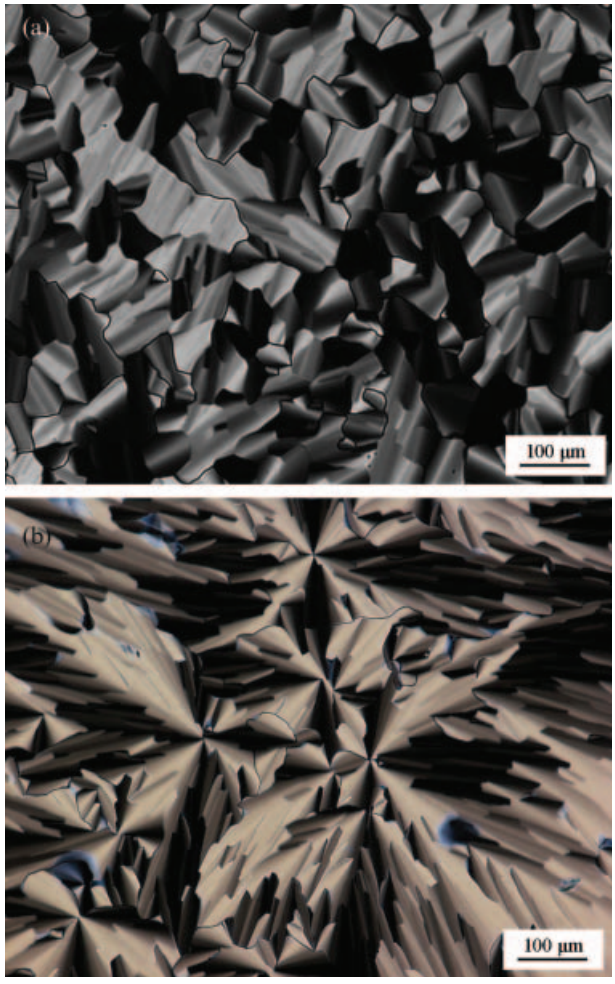

Figure 11. Optical micrographs between crossed polarisers of (a) caesium sulfonate **8** at 120°C and (b) pyridinium sulfonate **9** at 100°C after cooling from the isotropic melt.

mesophase can manifest its intrinsic structure (*28*). In the high temperature phase of the potassium salt **7** and in the single mesophase of the caesium sulfonate **8** similar kinds of spherolithic textures were observed. Spheroliths can be formed in smectic as well as in columnar hexagonal phases. In Figures 7 (b) and 11 (a), two different types of defects can be detected. First, the ends of all four cones of a spherolithic domain point towards its centre. In the columnar phase, molecular columns inside the flowerlike domains lie parallel to the glass substrate and bend into circles around the brush centres or emerge radially from the central defect (*29*). The second type of defect, which can be a signature of a columnar phase, is the so-called ''developable domain'' (*30*), expressing that the two pairs of cones do not contact at the central point of a spherolite (cf. centre of Figure 7 (b)). Developable domains result from the specific topology of hexagonal columnar phases and are highly indicative for this type of phase (*31, 32*).

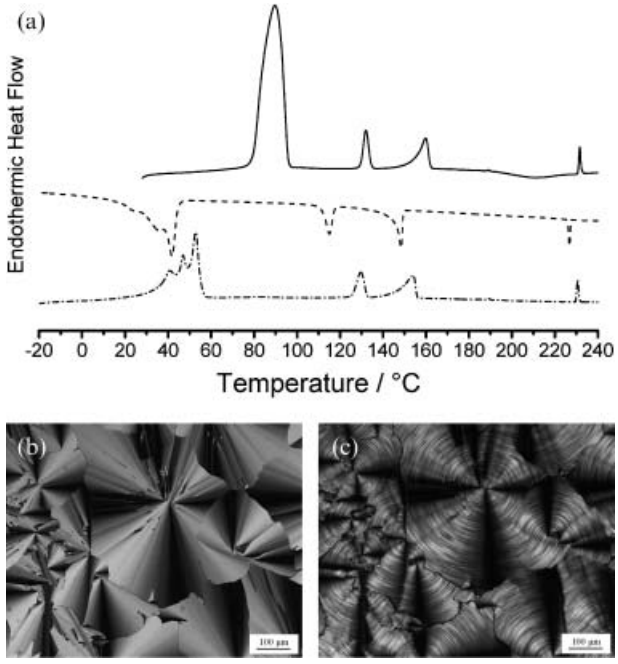

Figure 12. (a) DSC thermograms (— first heating, −··− second heating, --- cooling scan) and optical micrographs of tetramethylammonium sulfonate **10a** between crossed polarisers at 180°C (b) and 100°C (c) after cooling from the isotropic melt.

Since neither conic focal domains nor oily streaks have been found that originate from topological defects observed in some smectic mesophases (*33*), the texture observations make the presence of columnar mesophases probable. Furthermore, it is known from previous studies that wedge-shaped (tapered) amphiphiles frequently prefer to self-assemble into columnar mesophases (*34*).

A series of tetraalkylammonium 2,3,4-tris(dodecyloxy)benzenesulfonates has been prepared to generate amphiphiles with large polar head groups. The tetramethylammonium salt **10a** exhibited three sequential mesophases (Figure 12 (a)), i.e. the DSC thermogram resembled that of the potassium salt **7**. On cooling from the isotropic melt, compound **10a** showed a spherolithic-type texture that is frequently found with columnar mesophases (Figure 12 (b)). On further cooling below 160°C, the texture changed by developing a pattern of concentric black arcs around the centre of each spherolith, as depicted in Figure 12 (c). Such changes are known to be characteristic of the transition from one columnar mesophase into a columnar mesophase of higher degree of structural order, e.g. disordered/ordered ($Col_h \rightarrow Col_o$) or hexagonal/rectangular ($Col_h \rightarrow Col_r$) (*35*). The phase transition around 130°C did not alter the texture; only on crystallisation at 40°C did the

boundaries between the spheroliths become crumbled.

The tetraethylammonium salt **10b** melted at 126°C into the isotropic phase, but exhibited a monotropic mesophase that appeared at 98°C upon cooling from the isotropic melt. The clearing temperature could not be measured because of rapid crystallisation from the mesophase. The observed texture resembled a broken fan-shaped texture and the transition enthalpy of the mesophase formation I→Φ was rather small (0.3 kJ mol^{-1}). From these indications alone, the mesophase type cannot even be estimated.

Compound **10c**, a tetrabutylammonium salt, was a purely crystalline material with melting temperature of 81°C.

Four alkali metal salts were prepared from the symmetrically substituted 3,4,5-tris(dodecyloxy)benzenesulfonic acid, i.e. the lithium (**12**), sodium (**13**), potassium (**14**) and caesium (**15**) salts. According to the DSC thermograms and polarised optical investigations, the salts **12**–**15** all exhibited two sequential mesophases (see Figure 13). The clearing transitions were broad; hence the onset temperatures were lower than those of the respective asymmetrically substituted compounds, whereas the peak maximum temperatures were higher. Since the thermo-optically measured clearing temperatures were in general closer to the signal maximum temperatures, it seems to be justified to attribute higher clearing temperatures to the compounds **12**–**15**. The melt temperatures decreased from the lithium salt (T_m=52°C) to the potassium compound (T_m=−9°C), whereas the caesium salt melted at −3°C. Clearing temperatures could not be observed with compounds **12**–**14**, because these materials decomposed above 250°C prior to isotropisation. Only the caesium salt could be transferred in the isotropic melt on exceeding 200°C (see Table 2).

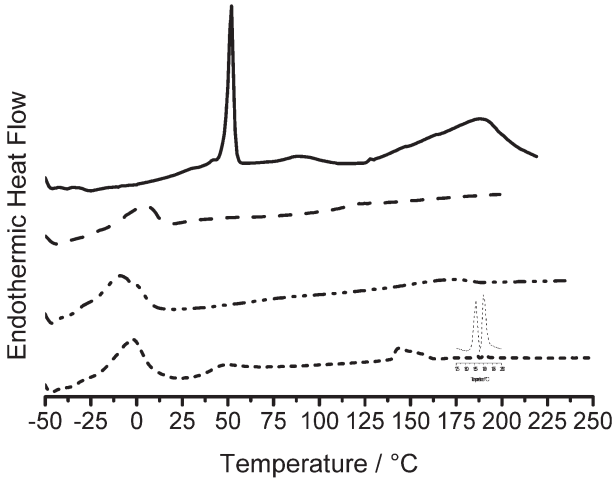

Figure 13. DSC thermogramms of the 3,4,5-tris(dodecyloxy)benzenesulfonates **12** (Li —), **13** (Na − − −), **14** (K −··−) and **15** (Cs ---).

Lithium, sodium and potassium salts decomposed without isotropisation, so it was not possible to generate textures by cooling from the isotropic melt. However, textures of the high temperature phases have been obtained from compound **12**, **13** and **14** on annealing at 180–200°C.

From the optical appearance of the textures of **12**–**13**, which contain elements of fan-shaped focal conic textures, as well as the needle like-textures of **15**, the formation of columnar mesophases isprobable (see Figure 14). The potassium sulfonate texture exhibited a mosaic-like pattern that still contained features from the low temperature phases (see Figure 14 (c)) and hence could not be consulted for the determination of the mesophase type of compound **14**.

On cooling the caesium salt **15** from 200°C at a rate of 10°C min^{-1}, a mosaic pattern texture of extremely low birefringence appeared below 190°C (Figure 14 (f)) that transformed below 139°C into a needle-like texture (see Figure 14 (e)).

Considering the symmetrically 3,4,5-substituted caesium salt **15**, the different substitution pattern caused a change of the phase behaviour, as followed from DSC and X-ray data. SAXS scans of caesium 3,4,5-tris(dodecyloxy)benzene sulfonate **15** at various temperatures are shown in Figure 15. The virgin sample revealed only one broad reflection with corresponding *d*-spacing of ~4.2 nm, whereas in the wide-angle region a set of reflections was found including the third, the fifth, the seventh and the ninth order of the abovementioned maximum, as well as some reflections at s>3 nm^{-1}. Based on the structural data for the very similar compound 3,4,5-tris(undec-10-enyloxy)benzenesulfonate (*36*) and for the abovementioned compound **8**, such an X-ray pattern can be attributed to an ordered columnar phase (C_{ho}) (Figure 16). Reflections 11 and 20 of the columnar phase are not observable possibly due to the low values of their structure factors. The SAXS curve of compound **15** did not practically change until 110°C, and starting from this temperature a shoulder at s ~2 nm^{-1} developed. Above 110°C, three reflections were observed, corresponding to d-spacings of d_{10}=3.1 nm, d_{11}=1.8 nm and d_{20}=1.5 nm, which definitely indicate the presence of a hexagonal disordered columnar mesophase (Col_{hd}), since no reflections at wide angles were observed. The transition from Col_{ho} to Col_{hd} was found to be reversible, as was verified by TOPM observations. After cooling

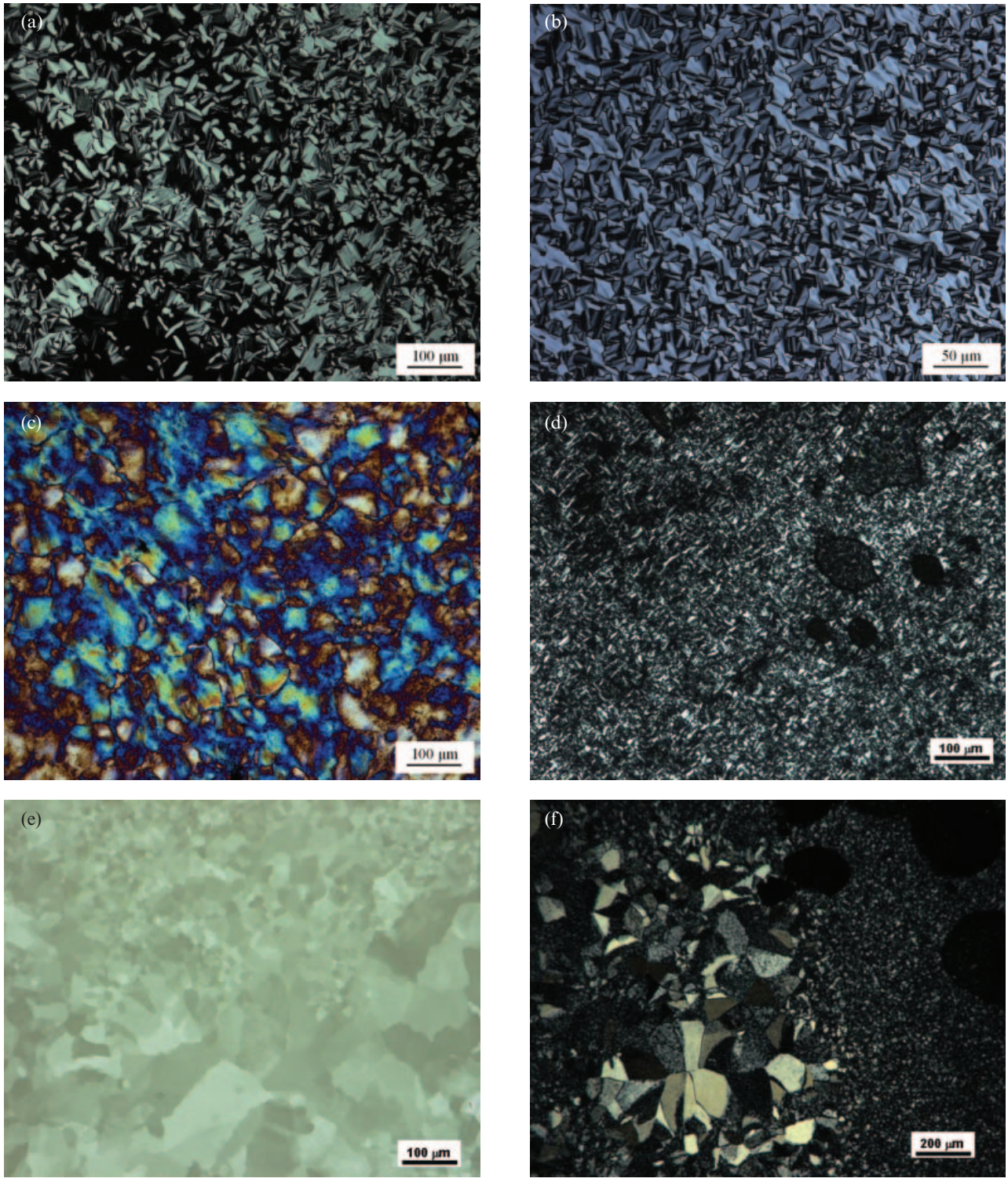

Figure 14. Optical micrographs between crossed polarisers of lithium salt **12** at 200°C (a), sodium salt **13** at 180°C (b), potassium salt **14** at 60°C (c) and caesium salt **15** at 138°C (d) and at 180°C (e) after cooling from the isotropic melt at 10 K min^{-1}. (f) Caesium salt **15** at 20°C after quenching from 200°C.

to room temperature at a rate of ~1°C min^{-1}, both Col_{ho} and Col_{hd} phases coexisted. The transition was found to be rather slow, because several days were required for the full transformation. Obviously the strong ion interactions in the centre of the columns slow down the transition kinetics. Upon storage at

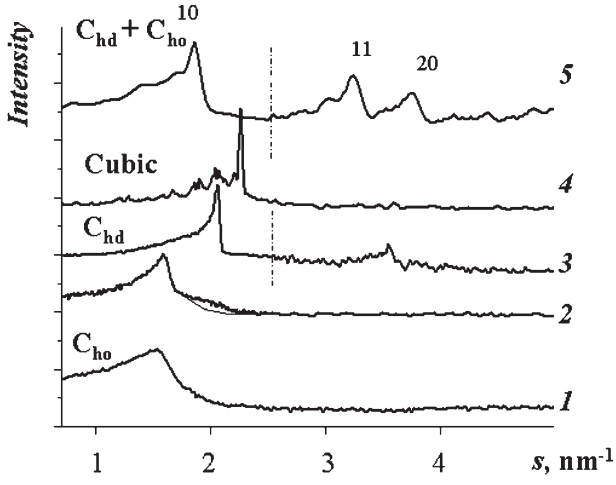

Figure 15. SAXS diffractograms of caesium 3,4,5-tris(dodecyloxy)benzenesulfonate **15**: as received at 20°C (1), heated to 125°C (2), 180°C (3), 230°C (4) and (5) after cooling to 20°C; tail part is multiplied by a factor of 5 and shifted.

ambient temperature the wide-angle X-ray pattern restored slowly as well.

The transition from the ordered to the disordered columnar phase leads to a strong redistribution of the electron density inside the columns, causing a drastic change in the relative intensities of diffraction reflections. In the ordered columnar phase the most intensive reflection was the 10 peak, and all other peaks made less then 0.5% of its intensity. On the other hand, the ratio of intensities of the first three reflections in the disordered columnar phase was I_{10}:I_{11}:I_{20}=1:0.06:0.02. It is important to underline that this substantial redistribution of reflection intensities is a characteristic feature of a transition from an ordered to disordered columnar phase for virtually all compounds studied (cf. curves 1 and 2 in Figure 8). The detailed analysis of such redistribution by means of electron density reconstruction will be the subject of a subsequent paper.

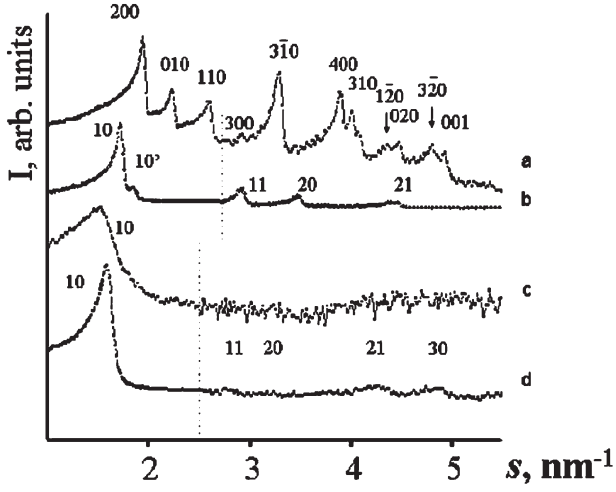

Figure 16. SAXS pattern of (a) caesium 2,3,4-tris(dodecyloxy)benzenesulfonate **8** at room temperature prior to first heating (''as prepared state''), (b) 2,3,4-tris(dodecyloxy)-benzenesulfonate **8** after cooling from the disordered columnar phase (C_{ho} phase prevails), (c) 3,4,5-tris(dodecyloxy)benzenesulfonate **15**; (d) 3,4,5-tris(undec-10-enyloxy)-benzenesulfonate. Tail parts are multiplied by a factor of 5 and shifted. Indices of observed reflections are shown.

Further temperature increase up to 190°C led to the development of a large grain structure characteristic to the formation of cubic plastic crystal mesophase (see the characterisation of compound **6**). The presence of a cubic phase at temperatures higher than 190°C was supported further by TOPM investigations showing the presence of optical isotropy.

Upon cooling down to 160°C, the disordered columnar mesophase was restored. Cooling further down to room temperature resulted in the development of an ordered columnar mesophase with a slightly lower cylinder diameter of 4.5 nm (Figure 9). As mentioned above, the disorder–order transition in the columns was kinetically hindered and took place over a period of several days. The cylinder diameter of the disordered columnar phase was 3.8 nm at 20°C.

The phase transition schemes of caesium 2,3,4-tris(dodecyloxy)benzenesulfonate **8** and caesium 3,4,5-tris(dodecyloxy)benzenesulfonate **15** are summarised in Scheme 4.

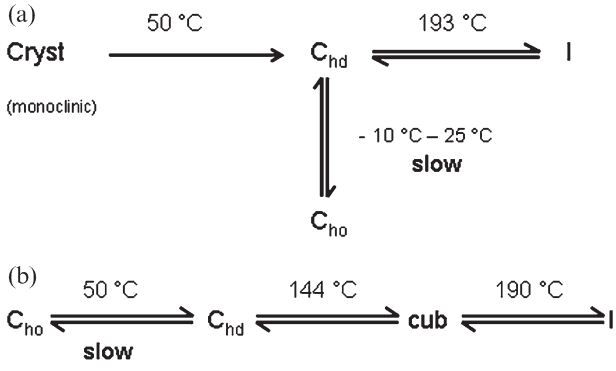

Scheme 4. Phase transition scheme of asymmetric (a) and symmetrically substituted (b) caesium tris(dodecyloxy)benzenesulfonates.

In contrast to compound **15**, sodium salt **13** is very sluggish in its phase transformations. Figure 17 shows the SAXS pattern of this material at room temperature. A complex set of reflections can be observed, which have been identified and indexed during the heating process, since different subsets of the reflections showed substantially different temperature behaviour. Two ''layer'' subsets are present, as well as the reflections of 2D hexagonal lattice. In accordance with the data obtained for the asymmetrical sodium 2,3,4-

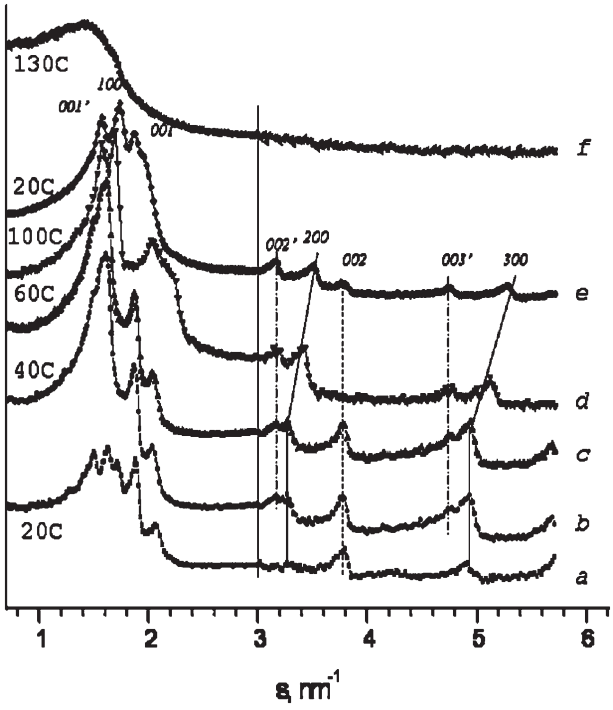

Figure 17. SAXS patterns of sodium 3,4,5-tris(dodecyloxy) benzene **13**: (a) as-received at 20°C, (b–d) heated up to 40, 60 and 100°C, respectively; (d) subsequent cooling to room temperature, (e) second heating above the isotropisation temperature at 120°C. Tail parts multiplied by 5 and shifted to previous positions for all plots.

tris(dodecyloxy)benzenesulfonate **6**, it was suggested, that two types of 3D hexagonal columnar lattice coexist in the sample. Upon heating, one of the meridional reflection sets gradually disappeared. It is interesting to note, that, whereas the *d*-spacings corresponding to the fibres repeat are substantially different in virgin phases (3.4 nm in compound **15** *vs* 4.2 mn in **6**), they become very close after the order–order transition (4.0 nm *vs*. 3.85 nm). The role of the bound water in the development of the virgin crystalline hexagonal phase, and of the release of this water in the order–order intracolumnar transition could be speculated in this respect, though we do not have enough data to make it a clear conclusion.

Comparison of the lattice parameters of the columnar phases exhibited by 2,3,4- and 3,4,5-tris(dodecyloxy)benzenesulfonates showed larger differences in the column diameters of the ordered phases (4.2 nm and 4.5 nm, respectively, for caesium salts, 3.6 nm and 4.2 nm for sodium salts) than for the disordered ones (3.9 nm and 3.8 nm for caesium salts). The models indicate that the different substitution pattern should affect the mutual positions of wedges in the ordered columnar phase more strongly than in the disordered situation.

It is important to underline the drastic differences of the columnar diameters found with the ordered phases formed by asymmetric 2,3,4-tris(dodecyloxy)-benzenesulfonates of caesium, sodium and lithium (4.2, 3.6 and 4.6 nm, respectively). This difference can be understood in terms of the numbers of molecules required to form the column repeat unit, resulting in different diameters of central ion channels. The irregular change of the column diameter with increasing metal ion size can be explained by a substantial difference in the internal arrangement of mesogen groups inside columns. This in turn is caused by the change in the shape of the mesogen group, responsible for the optimal packing of mesogens. The detailed structure of the mesophases formed by alkali 2,3,4- and 3,4,5-tris(dodecyloxy)-benzenesulfonates is the subject of a future paper.

Miscibility experiments

Miscibility experiments were performed within the sulfonate series to determine the mesophase type of other mesogens. According to the Arnold–Sackmann miscibility rule, two mesogens exhibit identical mesophases if the bordering regions of the two phases are connected by a continuous series of (liquid) mixed crystals (*37*). The binary phase diagrams of compounds **8/7**, **8/9**, **8/10a**, **8/15** and **8/16** were investigated by means of Kofler's contact preparation technique (*7, 38*). At a given temperature, the interdiffusion area represents a complete isothermal section of the phase diagram.

Figure 18 depicts a series of polarised optical micrographs of the mixtures of compound **8** and compound **10a**, together with the qualitative phase diagram was constructed from these pictures.

In this phase diagram, mixtures occur that exhibit higher isotropisation temperatures than both pure compounds (**8**: T_C=195°C, **10a**: T_C=231°C, maximum in mixture series: T_C^{max}=238°C), hence the presence of caesium ions stabilised the mesophase of the tetramethylammonium salt, and vice versa. As can be seen from Figure 18, above 170°C a continuous connection of mixed mesophases existed between the mesogens, hence the high temperature mesophase of compound **10a** is of hexagonal columnar type. The immiscibility between the low-temperature phases Φ_1 and Φ_2 of **10a** and the C_h phase of **8** is indicated by the fact that the changes in the morphologies of **10a** due to its phase transitions did not protrude in the second half of the contact zone.

Similar investigations of contact preparations demonstrated the miscibility of **8/7**, **8/9**, **8/15** and **8/16** in their mesophases. Hence, the mesophase of the

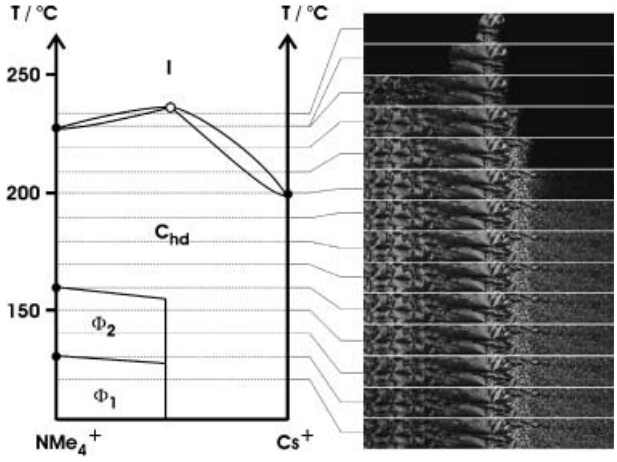

Figure 18. Schematic binary phase diagram of the mesogens **10a** and **8** together with polarised micrographs of the interdiffusion zone in a contact preparation of compound **10a** and compound **8**.

pyridinium salt **9** and the high-temperature phase of the potassium salt **7** are hexagonal columnar phases as well as the mesophases of the symmetrically substituted caesium salts **15** and **16**. Note, that on preparing the interdiffusion zone between **8** and **9** care must be taken not to overheat the pyridinium salt. Best results were obtained on annealing the preparation below 135°C, i.e. having it in contact the mesophase of **8** and the isotropic phase of **9**.

The occurrence of mesophases depends on the geometric shape of the mesogenic unit and the distribution of polar groups along the molecular skeleton. In particular with supramolecular mesogens the tendency of microphase segregation (*39*) and hence the amphiphilicity of the constituents of the supramolecular mesogenic unit are decisive if, and what type of mesophase can exist (*39*). For these reasons the relation between the mesophases of the sulfonate amphiphiles and their molecular architecture will be discussed.

At a given substitution pattern of the aromatic core the phase type and the transition temperatures are controlled by the size of the cation. In Figure 19 a the transition temperatures of the asymmetrically substituted sulfonates **5**–**10c** are plotted versus the radius of the respective cation; Figure 19 b depicts the analogous relationship for the symmetrically substituted compounds **12**–**15**. With the 2,3,4-substituted mesogens the graph is clearly separated into three domains: at cation radii below 0.12 nm only cubic phases are observed, whereas for intermediate cation sizes (0.15 nm$<r_{cation}<$0.27 nm) the hexagonal columnar mesophase dominates and with large cations ($r_{cation}>$0.35 nm) only crystalline phases exist. The compounds that represent the border between these domains (**7**:

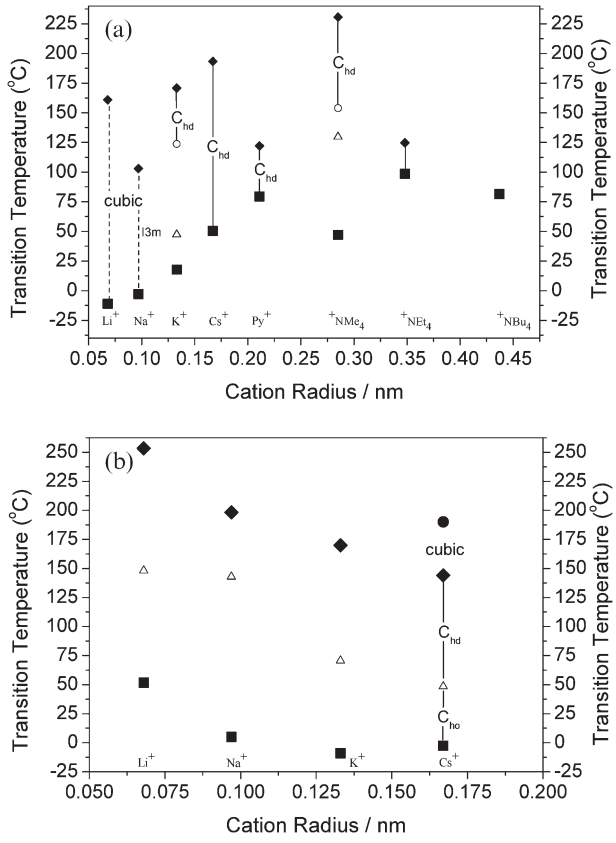

Figure 19. Plot of the transition temperatures of (a) 2,3,4-tris(dodecyloxy)benzenesulfonates and (b) 3,4,5-tris(dodecyloxy)benzenesulfonates versus the radius of the cation (■=melting temperature, ◆=isotropisation temperature, ○ and △=mesophase→mesophase transition temperatures).

cubic↔Col_{hd}, **10a**: Col_{hd}↔crystalline) exhibit a complex phase sequence of three subsequent enantiotropic mesophases, with the hexagonal columnar phase being the last phase before isotropisation. Note that similar relationships have been observed with other mesogenic homologues that show polymorphism if the phase type depends on variation of the molecular structure (*39, 40*). The overall tendency of the isotropisation temperatures is an increase with growing cation radius until $r_{cation}\approx$0.3 nm; above this value the clearing point falls short of the melting temperature, i.e. the mesophase becomes monotropic (**10b**). The pyridinium salt **9** does not perfectly fit in this scheme, most probably because the pyridinium ion is not a spherical but a flat ion. However, the dependence of the transition enthalpies on the cation radius supports the distinction of the three domains, in particular since the melting enthalpies of the two crystalline compounds **10b** and **10c** are about 3–4 times larger than the values of the mesogenes **5**–**9** (see Figure 20 (a)).

From a purely geometric point of view, small polar head groups should cause a cone-like shape of the

molecules that preferably assemble to spherical aggregates and arrange in lattices of cubic symmetry. Larger head groups generate molecules of truncated cone shape that prefer to organise into cylindrical superstructures and columnar phases. With very large cations, in particular the long-chain tetraalkylammonium ions that consist of a charged centre and an electro-neutral alkyl shell, it is possibly not required that the sulfonate mesogens form structures that confine the charged centres in their interior. However, at cation radii larger then 0.4 nm mesophases do not occur.

The transition temperatures of the symmetrically substituted sulfonates are depicted in Figure 19 (b). Both, the melting temperatures as well as the isotropisation temperatures show a minimum behaviour when plotted against the cation radius. Opposite to the asymmetrical sulfonates, the temperatures decrease from the lithium to the potassium salt, representing the minimum of the series. The subsequent caesium salt **15** exhibits more complicated behaviour; at T above 140°C the disordered columnar phase transforms to a cubic mesophase and then at $T \approx 190$°C the isotropisation occurs. The enthalpies continuously rise from the sodium to the caesium salt (cf. Figure 20 (b)), whereas the values of the melting enthalpy seem to exhibit a maximum with the potassium compound.

Summary

Two series of wedge-shaped tris(dodecyloxy)benzenesulfonate amphiphiles have been prepared and characterised with respect to their mesophases. From the dependence of transition temperatures and enthalpies on the cation diameter it is conclusive that the occurrence of mesophases with these compounds is more ruled by the geometric shape of the mesogen than by the ionic interactions between cation and sulfonate anion.

Depending on the diameter of the cation the asymmetrically substituted compounds **5**–**10a** exhibit cubic and columnar mesophases; the cubic symmetries are limited to cations of small size. Compounds with larger diameters exhibit columnar mesophases as long as the cation radius is below 0.35 nm, on exceeding this value only crystalline materials are obtained. Temperature dependent SAXS measurements revealed a negative thermal expansion coefficient with the example of the caesium salt **8**.

4. Conclusion

The sulfonate mesogens presented in this work represent a new example of wedge-shaped amphiphiles that form thermotropic columnar mesophases among wedge-shaped crown ethers (*19*), carboxylates (*33*), amides (*22*), diols (*40*) and others (*8*). Since all these compounds, though different in chemistry but similar in molecular geometry, form mesophases looking alike in structure (wedge centre located in the columns centre) and physical properties we propose to introduce the term 'cunitic' molecules[1] as a new descriptive term referring to wedge-shaped molecules and their mesophases.

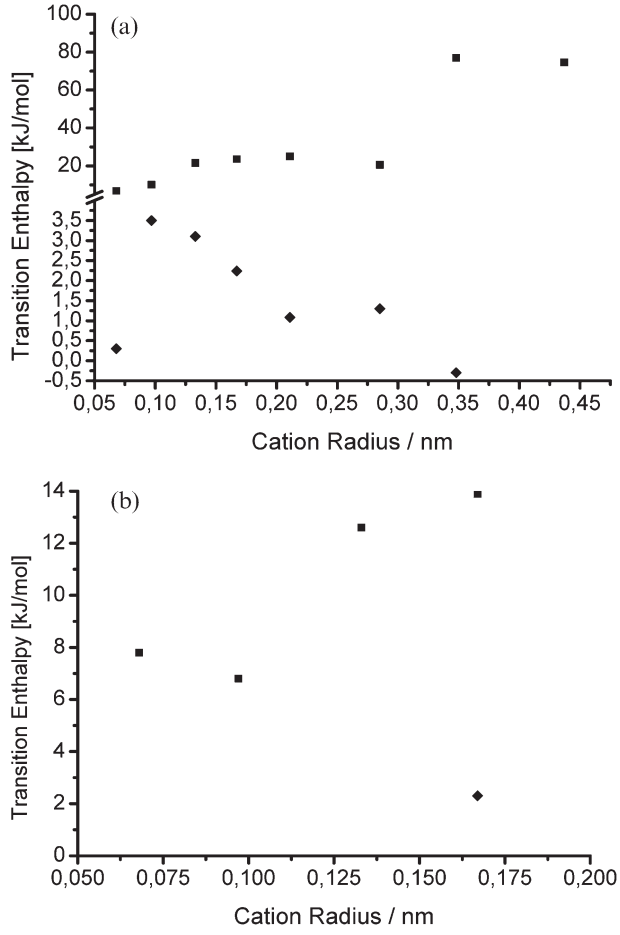

Figure 20. Plot of the melting and isotropisation enthalpies of (a) 2,3,4- and (b) 3,4,5-tris(dodecyloxy)benzenesulfonates (■=melting enthalpy, ◆=isotropisation enthalpy).

References

(1) Anonymous. *Plast. Additives Compounding* **2001**, *3*, 30–34.
(2) Kimura T.; Ito E. *Mater. Res. Soc. Symp. Proc.* **2000**, *598*, BB3.1/1–BB3.1/5.
(3) Ray S.S.; Okamoto M. *Prog. Polym. Sci.* **2003**, *28*, 1539–1641.

[1] Calamitic: (lat.) calamus=rod/pen, discotic: (lat.) discus=disc, cunitic: (lat.) cuneus=wedge.

(4) Garrett R.H.; Grisham C.M. *Principles of Biochemistry*; Harcourt College Publishers: Fort Worth, 2002.
(5) Steed J.W.; Atwood J.L. *Supramolecular Chemistry: A Concise Introduction*; John Wiley & Sons: Chichester, UK, 2000.
(6) Gokel G.W. *Advances in Supramolecular Chemistry*; Cerberus Press, Inc: South Miami, 2003, Vol. 9.
(7) (a) Borisch K.; Tschierske C.; Göring P.; Diele S. *Chem. Commun.* **1998**, 2711–2712; (b) Borisch K.; Diele S.; Göring P.; Kresse H.; Tschierske C. *J. Mater. Chem.* **1998**, *8*, 529–543.
(8) Beginn U. *Prog. Polym. Sci.* **2003**, *28*, 1049–1105.
(9) Percec V.; Peterca M.; Sienkowska M.J.; Ilies M.A.; Aqad E.; Smidrkal J.; Heiney P.A. *J. Am. Chem. Soc.* **2006**, *128*, 3324–3334.
(10) Beginn U.; Zipp G.; Möller M. *Chem. Eur. J.* **2000**, *6*, 2016–2023.
(11) Beginn U.; Zipp G.; Mourran A.; Möller M. *Mater. 12*, 513–516.
(12) Beginn U.; Weinmann S.; Möller M. *Chem. Engng Commun.* **2005**, *192*, 1116–1128.
(13) Yoshio M.; Kagata T.; Hoshino K.; Mukai T.; Ohno H.; Kato T. *J. Am. Chem. Soc.* **2006**, *128*, 5570–5577.
(14) Percec V.; Dulcey A.E.; Balagurusamy V.B.; Miura Y.; Smidrkal J.; Peterca M.; Nummelin S.; Edlund U.; Hudson S.D.; Heiney P.A., et al. *Nature* **2004**, *430*, 764–768.
(15) Mauritz K.A.; Moore R.B. *Chem. Rev.* **2004**, *104*, 4535–4585.
(16) Zhu X.; Tartsch B.; Beginn U.; Moeller M. *Chem. Eur. J.* **2004**, *10*, 3871–3878.
(17) Zhu X.; Scherbina M.A.; Bakirov A.V.; Gorzolnik B.; Chvalun S.N.; Beginn U.; Möller M. *Chem. Mater.* **2006**, *18*, 4667–4673.
(18) (a) Weichold O.; Zhu X.; Beginn U.; Percec V.; Möller M. *Polym. Mater. Sci. Engng* **2004**, *91*, 202–203; (b) Moeller, M.; Zhu, X.; Albrecht, K.; Beginn, U.; Mourran, A.; Gallyamov, M.O.; Gearba, R.; Ivanov, D.A. *Polym. Mater. Sci. Engng* **2006**, *94*, 199–200.
(19) Percec V.; Ahn C.-H.; Bera T.K.; Ungar G.; Yeardley D.J.P. *Chem. Eur. J.* **1999**, *16*, 1070–1083.
(20) Tapia R.; Torres G.; Valderrama J.A. *Synth. Commun.* **1986**, *16*, 681–687.
(21) Veselinovic D.S.; Obradovic M.V.; Mitic S.S.; Djordjevic S.B.; Zakrzewska J.S. *Zh. Prikladnoi Spektrosk.* **1995**, *62*, 71–75.
(22) Beginn U.; Lattermann G. *Mol. Cryst. Liq. Cryst.* **1994**, *241*, 215–219.
(23) Chvalun S.N.; Shcherbina M.A.; Bykova I.V.; Blackwell J.; Percec V.; Kwon Y.K.; Cho J.D. *Polym. Sci. A* **2001**, *43*, 33–44.
(24) (a) Zamir S.; Singer D.; Spielberg N.; Wachtel E.J.; Zimmermann H.; Poupko R.; Luz Z. *Liq. Cryst.* **1996**, *21*, 39–50; (b) Fontes E.; Heiney P.A.; de Jeu W.H. *Phys. Rev. Lett.* **1988**, *61*, 1202–1205.
(25) (a) Sauer T. *Macromolecules* **1993**, *26*, 2057–2063; (b) Zamir S.; Singer D.; Spielberg N.; Wachtel E.J.; Zimmermann H.; Poupko R.; Luz Z. *Liq. Cryst*. **1996**, *21*, 39–50; (c) Fontes E.; Heiney P.A.; de Jeu W.H. *Phys. Rev. Lett.* **1988**, *61*, 1202–1205.
(26) Kwon Y.K.; Chvalun S.; Blackwell J.; Percec V.; Heck J.A. *Macromolecules* **1995**, *28*, 1552–1558.
(27) Wunderlich B. *Macromol. Symp.* **1997**, *113*, 51–65.
(28) Shiyanovskaya I.; Singer K.D. *Phys. Rev. B* **2003**, *67*, 035204/1–7.
(29) Frank F.C.; Chandrasekahar S., *J. Phys.* (Paris) **1980**, *41*, 1285–1288.
(30) Klemann M., *Rep. Prog. Phys.* **1989**, *52*, 555–654.
(31) Oswald P., *J. Phys. Lett.* (Paris) **1981**, *42*, L171–L174.
(32) Bouligand Y*J. Phys.* (Paris) **1980**, *41*, 1297–1306.
(33) Percec V.; Glodde M.; Bera T.K.; Miura Y.; Shiyanovskaya I.; Singer K.D.; Balagurusamy V.S.K.; Heiney P.A.; Schnell I.; Rapp A., et al. *Nature* **2002**, *419*, 384–387.
(34) (a) Boltenhagen P.; Lavrentovich O.D.; Kleman M. *J. Phys. II, Paris* **1991**, *10*, 1233–1253; (b) Kwon Y.K.; Chvalun S.; Schneider A.-I.; Blackwell J.; Percec V.; Heck J.A. *Macromolecules* **1994**, *27*, 6129–6132.
(35) (a) Chandrasekhar S. in *Handbook of Liquid Crystals,* Vol. 2B, Demus D., Goodby J., Gray G.W., Spiess H.-W., Vill V. (Eds), Wiley-VCH, 1998. p. 749; (b) Destrade C.; Foucher P.; Gasparoux H.; Huu Tin N.; Levelut A.M.; Malthete J. *Mol. Cryst. Liq. Cryst.* **1984**, *106*, 121–146.
(36) Beginn U.; Chvalun S.N.; Shcherbina M.A.; Bakirov A.V.; Möller M., 2007, unpublished results.
(37) Sackmann H.; Demus D. *Z. Phys. Chem.* **1963**, *222*, 143–160.
(38) Kofler L.; Kofler A.; Brandstätter M. *Thermo-Mikromethoden*; Verlag Chemie: Weinheim, 1954. p. 151.
(39) Pegenau A.; Hegmann T.; Tschierske C.; Diele S. *Chem. Eur. J.* **1999**, *5*, 1643–1659.
(40) Staufer G.; Schellhorn M.; Lattermann G. *Liq. Cryst.* **1995**, *18*, 519–527.